Mouse Models for the Neurodegenerative Lysosomal Storage Diseases Niemann-Pick Types C1 & C2 and Classical Late Infantile Neuronal Ceroid Lipofuscinosis.

by

Mukarram S. EL-Banna

A thesis submitted to the

Graduate School-New Brunswick

Rutgers, The State University of New Jersey

in partial fulfillment of the requirements

for the degree of

Masters of Science

Graduate Program in

Microbiology and Molecular Genetics

and

The Graduate School of Biomedical Sciences

University of Medicine and Dentistry of New Jersey

written under the direction of

Dr. Peter Lobel

and approved by

_____

_____

_____

New Brunswick, New Jersey

May, 2009

ABSTRACT OF THE THESIS

Mouse Models for the Neurodegenerative Lysosomal Storage Diseases Niemann-Pick Types C1 & C2 and Classical Late Infantile Neuronal Ceroid Lipofuscinosis.

By MUKARRAM S. EL-BANNA

Dissertation Director:
Dr. Peter Lobel

Use of mutant mice provides us with an excellent tool for investigation of lysosomal diseases such as classical late infantile neuronal ceroid lipofuscinosis (cLINCL) and Niemann-Pick types C1 and C2 (NPC1 and NPC2). These are recessive devastating disorders in children that predominantly affect the central nervous system and result in progressive neurodegeneration and early death. Suitable mouse models enable us to assess behavioral, pathological, cellular, and molecular abnormalities associated with disease and to determine the efficacy of different therapeutic approaches. In addition, these models can be used to study the underlying function of the normal genes

This thesis addresses the generation and characterization of mouse models for these diseases. These include creation of gene-targeted models for cLINCL and NPC2 diseases. Disease progression was monitored by assessing gross phenotype (weight), behavioral parameters such as trembling, gait analysis and survival. This and other analyses indicate that the gene targeted mice are good models for the human disease. We also created a mouse model with mutations in both *Npc1* and *Npc2*. Comparison of the single and

double deficient NPC mutants indicate that the NPC1 and NPC2 proteins function in a common pathway. We also created mutant mice that expressed different levels of tripeptidyl peptidase 1 (TPP1), the protein deficient in cLINCL. This allowed estimation of how much protein is necessary to achieve therapeutic benefits.

Immunohistochemistry serves an important role in studying these mouse models and determining the distribution of the normal proteins. This is especially important when looking at protein distributions within the brain following gene or enzyme replacement therapy. We describe development of procedures to visualize TPP1, NPC1, and NPC2 in mouse brain.

Dedication

This work is dedicated to my family.

Acknowledgements

I would like to thank Dr. Peter Lobel for his guidance and for serving as my mentor. He embodies all the characteristics of a true scientist who conducts his research meticulously and with honesty and integrity. I would also like to thank Dr. David Sleat for being a great role model and teaching me about his “theory, what is his”. Without his guidance, my work would not be possible. I would like to thank Dr. Jim Millonig and Dr. Ann Stock for serving on my thesis committee.

I would also like to thank all the past and present members of the Lobel laboratory for being like a family to me. They help to provide a perfect environment for the great science they strive to produce. I am proud to be part of these exemplary people.

Finally, I would like to thank my husband Ahmed Mohamed for his support, love and care. You are the reason I did this. I would also like to thank my wonderful parents Mohamed El-Banna and Hanan EL-Banna, for being so understanding and helpful with the two little ones. Thanks to my two little ones, Yasin and Ameen, who serve as my inspiration, and to my wonderful sisters for their great help. A special thanks to Patricia Soudani for all her love and support and help with everything.

Table of Contents

List of Tables

Figures

Abbreviations

AAV	Adeno-Associated Virus
ANCL	Adult Neuronal Ceroid Lipofuscinosis
CE	Cholesterol Ester
cLINCL	Classical Late Infantile Neuronal Ceroid Lipofuscinosis
CLN2	Ceroid Lipofuscinosis, Neuronal 2
CNS	Central Nervous System
CT	Computed Tomography
DNA	Deoxyribonucleic acid
EEG	Electroencephalogram
ERG	Electroretinogram
ES	Embryonic Stem Cells
FA	Unesterified Fatty Acid
Glut	Gluteraldehyde
GM2	Ganglioside 2
GM3	Ganglioside 3
GSH	Glutathione
HIER	Heat Induced Epitope Retrieval
HMG-CoA	3- hydroxy-3-methylglutaryl CoA reductase
IgG	Immunoglobulin G
INCL	Infantile Neuronal Ceroid Lipofuscinosis

JNCL	Juvenile Neuronal Ceroid Lipofuscinosis
KCl	Potassium Chloride
LDL	Low Density Lipoprotein
LINCL	Late Infantile Neuronal Ceroid Lipofuscinosis
MAW	Methanol/Acetone/Water
NaCl	Sodium Chloride
NCL	Neuronal Ceroid Lipofuscinosis
NPA	Niemann-Pick type A
NPB	Niemann-Pick type B
NPC	Niemann-Pick type C
NPC1	Niemann-Pick type C-1
NPC2	Niemann-Pick type C-2
OCT	Optimal Cutting Temperature
PBS	Phosphate Buffered Saline
PFA	Paraformaldehyde
SAP	Saposins
SCAP	Sterol regulatory element- binding protein cleavage activating protein
SCMAS	Subunit c of the mitochondrial ATP synthase
SDS	Sodium Dodecyl Sulfate
TPP1	Tripeptidyl-peptidase 1
VER	Visual Evoked Response
VLINCL	Variant Late Infantile Neuronal Ceroid Lipofuscinosis

Introduction

Lysosomal storage disorders are comprised of a group of over forty genetic disorders in humans that result from defects in the function of the lysosome (Winchester et al., 2000). Lysosomes are organelles within the cytoplasm of the cell that contain enzymes, the majority of which are acid hydrolases, that break down substrates, such as lipids and proteins, into peptides, monosaccharides, amino acids, fatty acids, and nucleic acids (Figure 1). Diseases are due to the lack of one of these important enzymes thereby resulting in an accumulation of material within lysosomes.

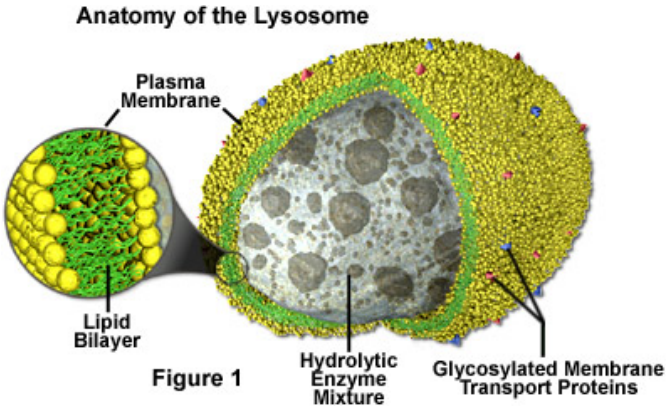

Figure 1: From http://micro.magnet.fsu.edu/cells/lysosomes/lysosomes.html

Lysosomal storage diseases are classified by type of primary stored material involved. Diseases include lipid storage disorders or lipidoses, such as Gaucher's and Niemann-Pick diseases, gangliosidosis (Tay-Sachs disease), glycoprotein storage disorders, and mucolipidoses. There currently are no cures for these diseases; however there have been

studies involving bone marrow transplantation and enzyme replacement therapies that show some progress in treatment options (Bruni et al., 2007; Clarke and Iwanochko, 2005). Gene therapy may also be an option in the near future (Passini et al., 2006; Ponder and Haskins, 2007). In our laboratory we currently have mouse models for classical late infantile neuronal ceroid lipofuscinosis (cLINCL) and Niemann-Pick C (NPC) types 1 and 2. Investigation of lysosomal storage disorders such as cLINCL and the NPC types 1 & 2 require the utilization of mouse models in order to aid in elucidating the specific localization of proteins associated with these diseases. Key to understanding the NPC and TPP1 proteins is to have definitive understanding of their localization within cells. In this laboratory, we have become progressively experienced in determining the best possible methods for localization of these proteins using cryo-preserved tissues and immunohistochemistry. Here we give a detailed description of the techniques used in fixation, cryo-preservation and staining of mouse tissues, primarily mouse brain. It is the aim of this study to achieve optimal morphological preservation of samples as well as quantitative assessment and reproducibility of the cLINCL and NPC associated lysosomal proteins. This will help in subsequent studies involving replacement of enzymes or proteins that are missing or deficient in these diseases. It will provide us with a reliable method to visualize spread and localization of supplemented therapeutic substances.

1. Neuronal Ceroid-Lipofuscinosis (NCLs)

The neuronal ceroid-lipofuscinoses (NCLs) constitute one of the most common types of genetic neurodegenerative diseases affecting children (Zeman and Dyken, 1969). Incidence in the US alone has been estimated to be at 1:12500 (Rider and Rider, 1988) and disease is usually of the autosomal recessive type. Age of onset of these diseases can be anywhere from early infancy to late adulthood. Childhood forms are characterized by progressively frequent and severe seizures and vision loss followed by premature death while adult forms are mostly seen as displaying dementia. Vision loss is often an early sign of NCL and can be detected in three of the childhood forms. However, because vision loss occurs in other eye diseases as well, the disease cannot be diagnosed by this abnormality alone. Various other diagnostic tests have to be used in order for a definite diagnosis to be made. These tests include: Electroencephalogram (EEG) tests for recording brain currents and brain electrical activity to determine whether a patient experiences seizures and visual evoked responses (VER) as well as electroretinograms (ERG) to detect various eye problems that are usually associated with NCL. There is also skin/tissue sampling where a biopsy of either is examined under an electron microscope to help spot typical NCL deposits. These deposits can be seen in various tissues such as skin, conjunctiva, muscle, rectal etc. as well as blood (Haltia, 2003). There are also enzyme assays available as a recent development in the diagnosis of NCL, which look for specific lysosomal enzymes that are missing in infantile and late infantile forms only. Computed tomography (CT) scans can also be used to scan the brain for any structural abnormalities such as areas of brain atrophy that are commonly seen in NCL patients.

Classification of the various forms of this disease is not as self-explanatory as one might think. As a result, a sub classification has emerged that is based on the age of onset of the disease as well as the type and structure of the storage material. As a result, three main forms have been recognized. These are infantile (INCL), late infantile (LINCL) and juvenile (JNCL) (Haltia, 2003). Recent advances in biochemical and genetic research have transformed the way these diseases are classified. The NCLs are now classified into 9 main genetic forms (Table 1), based on the number of gene loci.

The Human Neuronal Ceroid-Lipofuscinoses (NCL): Genetic Classification			
Gene	**Gene Product**	**Clinical Phenotype**	**Principal Stored Protein**
CLN1	Palmitoyl protein thioesterase 1	INCL (LINCL, JNCL,	SAP A & D
CLN2	Tripeptidyl peptidase 1	Classic LINCL	SCMAS
CLN3	CLN3 protein (membrane protein)	JNCL	SCMAS
CLN4	PPT1 protein	ANCL	SCMAS
CLN5	CLN5 protein	Finnish vLINCL	SCMAS
CLN6	CLN6 protein	vLINCL	SCMAS
CLN7	MFSD8 protein	Turkish vLINCL	SCMAS
CLN8	CLN8 protein (membrane protein)	Northern Epilepsy	SCMAS
CLN10	Cathepsin D	Congenital NCL	SCMAS

Table 1: Abbreviations INCL= infantile NCL; LINCL= late infantile NCL; vLINCL= variant late infantile NCL; JNCL= juvenile NCL; ANCL= adult NCL; SAP= saposins; SCMAS = subunit c of the mitochondrial ATP synthase.

2. Classical Late-Infantile Neuronal Ceroid Lipofuscinosis (cLINCL), Biochemical Features and Neuropathology

Mutations of the TPP1 gene (also called *CLN2*, for ceroid lipofuscinosis neuronal 2) are responsible for all cases of classical late infantile NCL (cLINCL) (Haltia, 2003). Clinical features of cLINCL are usually observed between 2 and 4 years of age and are manifested as seizures. These seizures may be partial, generalized tonic-clonic, or secondarily generalized and are soon followed by ataxia, myoclonus, and developmental regression, with patients becoming unable to walk or sit unsupported and losing speech (Haltia, 2003). There is a gradual loss of vision that ends in blindness at age 5 or 6 years and patients usually die in middle childhood (Haltia, 2003; Wisniewski et al., 2001). At autopsy, the brain, particularly the cerebellar area, is severely deteriorated with brain weights typically being 500 to 700 g, about half that of an unaffected individual (Elleder and Tyynela, 1998).. Cutting through the brain reveals enlarged ventricles and a thinner cortex (Haltia, 2003). Examination by light microscopy reveals a severe loss of cerebral cortical neurons and activation of the micro- and macroglia (Haltia, 2003). Cerebellar Purkinje cells and granule cells are severely reduced in number and the cytoplasm of the remaining perikarya in the cerebral cortex and subcortical structures is slightly to moderately enlarged with storage granules (Haltia, 2003). Meganeurites or spindle-shaped accumulations of storage granules in the proximal axonal segments of cortical neurons, are also a characteristic feature (Haltia, 2003). Myoclonus bodies, or spheroids, may occur in the neurons of the basal ganglia and dentate nucleus (Elleder and Tyynela, 1998). Neuronal loss is accompanied by a secondary loss of axons and myelin in the

white matter (Haltia, 2003). There is atrophy of the retina which is more apparent in the peripheral than in the central area and begins at the photoreceptor layer (Elleder and Tyynela, 1998). Observed storage granules are autofluorescent in nature and stain with Luxol fast blue, PAS, and Sudan black B in paraffin prepared sections. These granules are highly immunoreactive for subunit c of mitochondrial ATP synthase (SCMAS) (Lake and Hall, 1993) as well as for SAP-A and SAP-D (Tyynela et al., 1995). Minor deposits of similar granules are also evident in astrocytes as well as many other cell types throughout the body. These storage bodies have a uniform ultrastructure in all cells that are involved and are bound by a unit membrane. They consist of accumulations of curvilinear profiles that are curved short thin lamellar stacks of alternating dark and light lines that range in dimension from 1.9 to 2.4 nm. Granular or fingerprint components are not observed and SCMAS has been shown to be the major protein component of purified storage material (Palmer et al., 1992), (Tyynela et al., 1997).

3. Molecular Genetics of *CLN2*

CLN2 was mapped to chromosome 11p15 using homozygosity mapping in consanguineous families (Sharp et al., 1997). The gene product and the gene itself were identified using a biochemical approach (Sleat et al., 1997). The *CLN2* gene encodes a ubiquitously expressed lysosomal protease with tripeptidyly-peptidase I activity (TPP1) (Rawlings and Barrett, 1999; Sleat et al., 1997; Vines and Warburton, 1999). There have been over 64 different mutations of this gene reported (www.ucl.ac.uk/ncl/#). There are two mutations which are particularly common, IVS5-1G->C where splicing is affected and R208X, a nonsense mutation (Sleat et al., 1999; Zhong et al., 1998).

4. Genetically Engineered Mouse Models of cLINCL; the *Cln2*-targeted mouse and the *Cln2* hypomorphs

4a. *Cln2*-targeted mouse model

Our laboratory, (Sleat et al., 2004a) generated and characterized the first *Cln2*- targeted mouse model for cLINCL. The murine *Cln2* gene is located within mouse chromosome 7 where the Cln2 gene sequence is located. This was used to amplify long and short arms from 129SvEv genomic DNA. The 1.9kb short arm, nucleotides 119277-121171, of chromosome 7 clone AC121823, was cloned as a *Bgl*II fragment into the *Bam*HI site of pTK-LNL (obtained from Richard Mortensen, University of Michigan, Ann Arbor, MI), a targeting vector, containing thymidine kinase for negative selection and a lox-P flanked neo cassette for positive selection. The 4.8 kb long arm corresponding to nucleotides 114520-119276 of AC121823, was engineered to harbor a point mutation of (G119096A of AC121823) that was predicted to change amino acid 446 of the murine Cln2 gene product from arginine to histidine corresponding to the late-onset human mutation Arg447His (Sleat et al., 1999). The long arm was inserted into the *Sal*I site of pTK-LNL, and the targeting plasmid was linearized with *Not*I to eliminate bacterial plasmid derived DNA (Sleat et al., 2004a). Targeted ES cells were selected for and injected into C57BL/6 blastocytes that were then implanted into pseudopregnant Swiss-Webster females using standard techniques. Resultant chimeric offspring were then bred with C57BL/6 females generating a number of offspring that were heterozygotes for the allele of interest (Cln2)

and which were confirmed to be as such by Southern blotting. Subsequent genotyping is performed by utilizing the polymerase chain reaction using a set of three primers (ATCTGATGGCTACTGGGTGG, CCGGTAGAATTCCGATCAT, and CCCCCAAACACTGGAGTAGA) that produce 402 nucleotide (wild-type) and 328 nucleotide (targeted) products. The *Cln2* phenotype seen in these mice results from a combination of an Arg446His missense mutation as well as a splicing defect that is a result of the insertion of a floxed neo selection marker (Figure 2 from (Sleat et al., 2008)). This mouse model for *Cln2* recapitulates the features of cLINCL with accumulation of storage material that shows the classic curvilinear profile ultrastructure as well as a rapid neurodegenerative phenotype with mice dying at 138d with 90% of the mice being found dead between days 108 and 169. When in an isogenic 129 SvEv background, life-span was longer, median being 164d and 90% death between 136 and 185d, thereby indicating the possible presence of strain specific modifier(s) of the *Cln2* phenotype (Figure 3 from (Sleat et al., 2004a)). This mouse exhibits the earliest onset with the most pronounced neurodegenerative phenotype of any NCL mice (Cooper et al., 2006). It is apparent that degeneration is pronounced within the thalamocortical system of these TPP1-deficient mice, with marked effects seen within the cerebellum (Sleat et al., 2004a). These mice were then backcrossed 10 generations into C57BL/6 to achieve an isogenic background for use in further studies including evaluation of potential therapies for cLINCL. In addition, the TPP1-deficient mice serve as a critical negative control for immunohistochemical characterization of the *Cln2* protein tripeptidyl peptidase 1(TPP1) and its localization and expression in mouse brain.

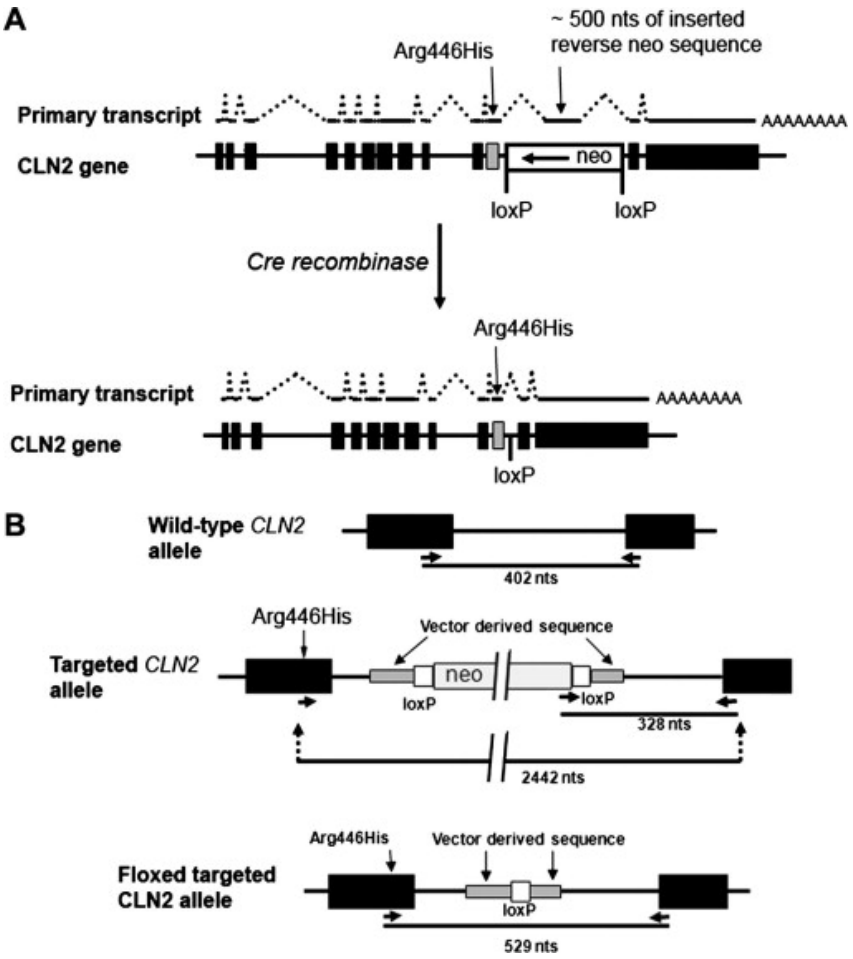

Figure. 2. From Sleat et al 2008. *CLN2* hypomorph construct. (A) The *CLN2*-targeted allele was originally generated by the synergistic combination of an Arg446His allele with the insertion of a neomycin selection cassette into intron 11 of the murine *CLN2* gene. This results in an unstable mRNA containing a ~500 nt reverse orientation neo insertion (Sleat et al., 2004a). The targeted *CLN2* alleles described in this study were generated by the cre-mediated excision of the neo marker. This resulted in transcription of a normally spliced and stable *CLN2* mRNA that differs from the wild-type transcript only in the presence of the missense mutation. (B) Details of the targeted *CLN2* allele and genotyping primer locations.

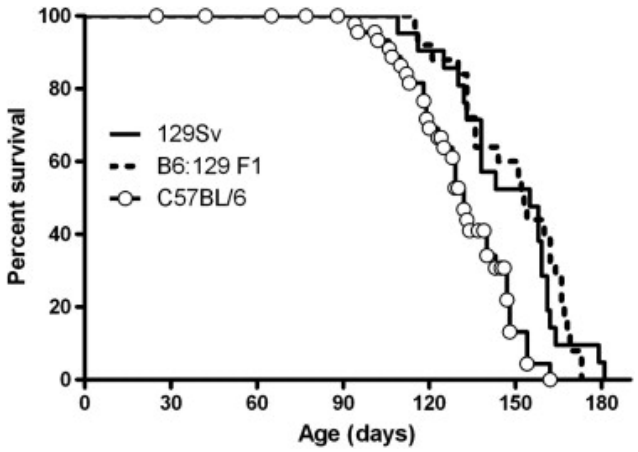

Figure.3. From (Sleat et al., 2008) Comparison of survival of the *CLN2*-mutant mice with different strain backgrounds. Mice were isogenic for either C57BL/6 or 129SvEv genetic background or were a first generation cross between these strains. 129Sv, $n = 21$; C57BL/6, $n = 33$, 129Sv × C57BL/6 F1, $n = 25$

4b. *Cln2*-hypomorph mouse model

The *Cln2*-hypomorph was generated in our lab by crossing male *Cln2* heterozygous mice (*Cln2* +/-) with female Zp3-cre mice (The Jackson Laboratory, Bar Harbor, Maine) resulting in the removal of the neo selection marker in the offspring of these mice (Sleat et al., 2004a). The female *Zp3-cre* mice are a transgenic line in a C57BL/6 background that expresses cre within the oocyte from the zona pellucida 3 gene promoter (de Vries et al., 2000). Progeny were then screened for cre-mediated excision of neo using primers (ATCTGATGGCTACTGGGTGG, CCCGGTAGAATTCCGATCAT, and CCCCCAAACACTGGAGTAGA) that produced 402 nucleotide (wild-type) and 328 nucleotide (targeted) products as well as a 529 nucleotide product from the mutant allele (targeted allele) after neo excision (Figure 2 from (Sleat et al., 2008)). Mice that were heterozygous for the neo excision (+/f) were backcrossed against C57BL/6 mice and were selected for loss of the cre transgene using a primer set (GCGGTCTGGCAGTAAAAACTATC and GTGAAACAGCATTGCTGTCACTT)

which results in a 100-nucleotide product. This mouse hypomorph was generated in order to determine what levels of TPP1 activity are necessary in order to achieve an ameliorative effect when attempting to treat the disease. The life span of this mouse (*Cln2* hypomorph or f/f) was shown to be nearly 4 times that of the *Cln2* -/- mouse (Figure 4 from (Sleat et al., 2008)).

This mouse will be used to provide us with beneficial threshold levels of activity for future therapeutic approaches. Mice were backcrossed 10 generations into C57BL/6 to achieve an isogenic background for use in further studies including immunohistochemical characterization and localization of the *Cln2* protein tripeptidyl peptidase 1 (TPP1) and its expression in the brain of these hypomorphs.

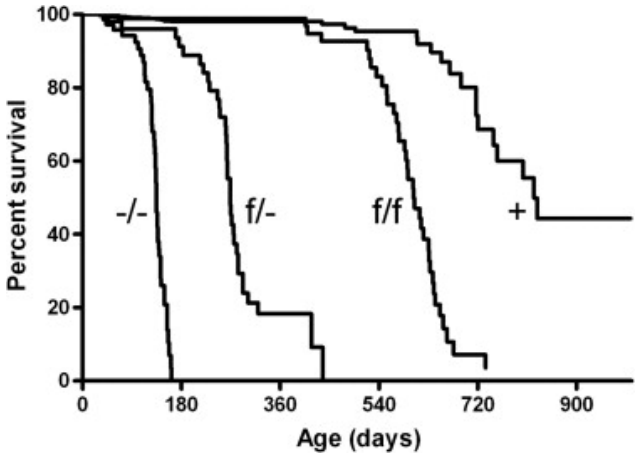

Figure. 4. From (Sleat et al., 2008) Survival analysis of *CLN2*-mutants. Mice were in either congenic or near congenic (≥6 backcrosses) C57BL/6. Data represent the following numbers of mice: −/−, *n* = 47; f/−, *n* = 35; f/f, *n* = 36; control +, *n* = 33 (+/−, *n* = 15; +/+, *n* = 5; +/f, *n* = 13).

5. Potential avenues for therapeutic intervention in cLINCL disease using our mouse models

The mouse model provides an excellent tool for investigation of molecular mechanisms underlying cLINCL and the resulting devastating disorder that affects the largely inaccessible tissues of the central nervous system. Our mouse models enable us to assess behavioral, pathological, cellular, and molecular abnormalities as well as allow for the development of novel therapies for a thus far incurable disease. The *Cln2* hypomorph mouse model provides us with the TPP1 levels needed in order to significantly affect the progress of this disease as well as enlightens us with the necessary starting point for further studies using various therapeutic approaches such as chemical chaperone therapy, enzyme replacement therapy, neural stem cell therapy, gene therapy, convection-enhanced delivery of proteins, hematopoietic stem cell therapy (cord blood transplant), and genetically modified cell therapy (Hobert and Dawson, 2006).

With the introduction of our mouse model for cLINCL, it was possible for this therapeutic approach to be tested. Previous studies in normal rodents and nonhuman primates showed that expression of human TPP1 protein could be expressed in the brain following intracranial injection of recombinant AAV vectors that contained the human CLN2 cDNA (Haskell et al., 2003; Sondhi et al., 2005). Those studies also demonstrated that human TPP1 protein is secreted by transduced cells and taken up by neighboring cells via receptor-mediated endocytosis, similar to that observed for other lysosomal enzymes (Neufeld, 1991). Our TPP1-deficient mice have recently been used in an attempt at *Cln2* (*Tpp1)* AAV mediated gene therapy that resulted in a significant reduction in storage material and prolonged survival of these mice (Cabrera-Salazar et al., 2007;

Passini et al., 2006; Sondhi et al., 2007; Sondhi et al., 2008). It is believed that patients with cLINCL may benefit from gene therapy due to the fact that it is a monogenic disease. The introduction of a functional version of the *Cln2* gene to the brain via intracranial injection of a viral vector may remove storage material and rescue cells from dysfunction (Cabrera-Salazar et al., 2007; Passini et al., 2006; Sondhi et al., 2007; Sondhi et al., 2008). This type of strategy has been shown to be effective in other mouse and cat models with lysosomal storage disorders treated with adeno-associated virus (AAV) vectors (Bosch et al., 2000; Frisella et al., 2001; Matalon et al., 2003; Passini et al., 2005; Passini et al., 2003; Sferra et al., 2000; Skorupa et al., 1999).. The information obtained from this gene-therapy approach using intracranial delivery of CLN2 to reduce brain pathology in a mouse model of cLINCL provided proof that the delivery of human CLN2 cDNA to the diseased brain is a promising strategy for treating this disease (Cabrera-Salazar et al., 2007; Sondhi et al., 2007). Mice had significant reduction in CNS storage granules and demonstrated improvement in gait, nesting, seizures, balance beam results, and grip strength, as well as exhibited prolonged survival (Sondhi et al., 2007). This type of treatment has very good potential for implementation in the human patients with this disease as shown by (Worgall et al., 2008). Using immunohistochemistry and our mouse models, we will be able to track the expression or effect of any supplemented TPP1 protein used in any therapeutic approach to determine efficacy of the treatment.

6. Niemann-Pick C disease

Niemann-Pick type C (NPC) disease is an autosomal recessive disorder that is characterized by progressive neurodegeneration. Disease is caused by a mutation in one of two genes, the NPC1 gene (95% of the cases) or the NPC2 gene. NPC disease is distinct biochemically from the Niemann-Pick disease types A or B in that the later types are due to a genetic defect in sphingomyelinase activity (Brady et al., 1966). Clinical symptoms of NPC disease include vertical gaze palsy, ataxia, dystonia and seizures, and are usually seen in early childhood with death usually resulting in the teenage years. NPC infants show symptoms of neonatal liver enlargement, jaundice, and splenomegaly with a few individuals dying of acute liver failure. There is currently no effective treatment for NPC disease. Histological characteristics of the disease include neuronal loss, particularly that of the cerebellar Purkinje cells as well as the widespread appearance of swollen neurites (Higashi et al., 1993). Biochemically, the phenotype of NPC deficient cells and tissues is the lysosomal accumulation of cholesterol (Liscum et al., 1989; Sokol et al., 1988) and other lipids such as bis-monoacylglycerol phosphate (Kobayashi et al., 1999) and gangliosides GM2 and GM3 (te Vruchte et al., 2004; Watanabe et al., 1998; Zervas et al., 2001a). The brain, being the most cholesterol rich organ in the body, contains 25% of the body's cholesterol (Vance, 2006). In most tissues cholesterol is acquired through endogenous synthesis or through receptor mediated endocytosis of plasma lipoproteins such as low-density lipoproteins (LDLs) (Vance, 2006). Cholesterol metabolism in the central nervous system (CNS) is different because plasma lipoproteins are unable to cross the blood-brain barrier. Thus, all cholesterol in the brain is synthesized within the CNS

(Turley et al., 1996). In the brain of adult animals, the majority of cholesterol lies within myelin (70-80%) (Vance, 2006). High rates of cholesterol synthesis occurs in the brain during the period of active myelination which is then resultant in a decline in cholesterol synthesis to a level where it is thought to reflect mostly that which is occurring in neurons and astrocytes (Spady and Dietschy, 1983). The half-life of cholesterol in the brain is 4-6 months (Vance, 2006). For the maintenance of cholesterol homeostasis in the brain, the export of excess cholesterol in the form of 24-hydroxy cholesterol from the brain to the plasma must occur. (This derivative of cholesterol is produced by the action of cholesterol 24-hydroxylase which is a specific enzyme expressed in only a subset of neurons (Lund et al., 2003). It is interesting to note that cholesterol accumulation results in all tissues except the brain and that actual cholesterol levels are seen to decrease with age increase in NPC disease (Xie et al., 1999). This may be a result of the extensive demyelination that results from NPC disease (Takikita et al., 2004). Due to the fact that myelin is the major source of cholesterol in the brain, progressive loss of myelination would be expected to mask any age-related increase in cholesterol content of neurons and astrocytes. It was discovered that cholesterol is sequestered in the brains of mice with NPC disease but that turnover is increased (Xie et al., 2000). Furthermore, accumulation of cholesterol within neuronal lysosomes can be seen by histochemical staining (Distl et al., 2003). This finding supports the hypothesis that cholesterol does accumulate within the lysosomes of brain cells but cannot be seen biochemically because of cell death and demyelination.

7. *NPC* Genes

7a. *NPC1*

The human *NPC1* gene was identified and cloned in 1997 (Carstea et al., 1997). The NPC1 protein is an integral membrane protein that is primarily located in the late endosomes/lysosomes as well as in the Golgi complex (Higgins et al., 1999; Neufeld et al., 1999). This protein consists of 1278 amino acids and 13 putative transmembrane domains (Figure 5). It was discovered that the cholesterol-binding site is located at luminal loop-1, a 240-amino acid domain with 18 cysteines (Infante et al., 2008).

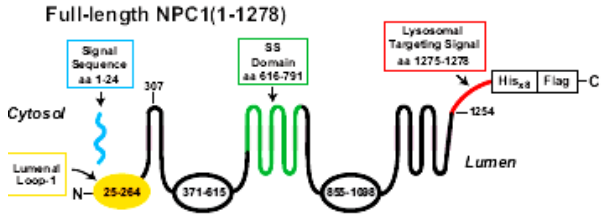

Figure. 5: From (Infante et al., 2008) Topological model of NPC1 protein, NPC1 is a 1278-amino acid transmembrane protein found in late endosomal/lysosomal membranes. The lumenal N-terminus of the protein contains a leucine zipper motif whereas the C-terminus is cytosolic and contains a lysosomal targeting sequence. The protein contains 13 transmembrane domains where five of these domains are involved in sterol sensing . Luminal loop 1 is shown in yellow and is where the NPC1 binds cholesterol.

Comment [CABM1]: Just make sure you realize that the his flag are synthetic additions to the recombinant protein that are used for purification/detection and are not found on the endogenous protein.

NPC1 also contains a cysteine-rich loop (Watari et al., 2000), a di-leucine lysosomal targeting motif and a leucine zipper (Watari et al., 1999a). An important feature of the NPC1 protein is the five transmembrane domains that comprise a sterol-sensing domain (Carstea et al., 1997; Watari et al., 1999b). This motif has previously been identified in other proteins that are involved in regulating cholesterol, such as the sterol regulatory element-binding protein cleavage activating protein (SCAP) and 3-hydroxy-3-methylglutaryl-Co-A reductase (Vance, 2006).

7b. ***NPC2***

The NPC2 gene (*HE1*) was identified in a study, conducted in our lab, which was designed to characterize the lysosomal proteome (Naureckiene et al., 2000). The NPC2 protein is comprised of 151 amino acids and is a ubiquitously expressed soluble protein that is present in the lumen of the lysosome. This cholesterol-binding protein had previously been identified in the epidydimis as a major secretory component of epididymal fluid (Okamura et al., 1999). Ko et al. used site directed mutagenesis to gain information about where the NPC2 cholesterol-binding site was (Ko et al., 2003). Friedland et al. determined the structure of free (non-cholesterol bound) NPC2 (Friedland et al., 2003). Later on, the crystal structure was solved and reveals a hydrophobic binding pocket that has the ability to bind cholesterol (Xu et al., 2007). Disease progression in patients affected with NPC2 appears to be the same as those who are affected with NPC1 (Klunemann et al., 2002; Vanier and Millat, 2004). The precise functions of both of these proteins have yet to be elucidated.

The availability of cell and animal models of deficiency has greatly aided investigation of these diseases. A hypomorphic mouse expressing 0-4% of residual NPC2 protein was generated in this lab (Sleat et al., 2004b) and it was observed that the progression of neurological symptoms and lipid accumulation in Npc1 -/- mice , Npc2 –hypomorphs as well as the double mutants of these mice were essentially identical thereby suggesting that both NPC1 and NPC2 take part in the same lipid pathway (Sleat et al., 2004b). This will be discussed in greater detail in a subsequent section.

8. NPC proteins are required for the egress of cholesterol from late endosomes/lysosomes

The accumulation of large amounts of unesterified cholesterol in late endosomes/lysosomes of NPC1 deficient fibroblasts that have been loaded with LDL-cholesterol implies that NPC1 is involved in the movement of LDL derived, unesterified cholesterol out of the endosomal pathway (Liscum et al., 1989; Sokol et al., 1988). This idea is further supported by the fact that the NPC1 protein contains a sterol-sensing domain (Carstea et al., 1997). The intracellular transport pathways for LDL derived cholesterol are illustrated in (Figure 6 from (Vance, 2006)).

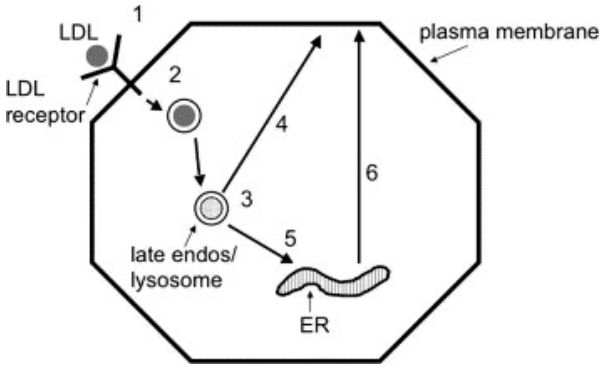

Figure. 6: From (Vance, 2006). NPC1 is involved in the movement of low-density lipoprotein (LDL)-derived cholesterol from late endosomes/lysosomes. (1) LDL is (2) endocytosed by LDL receptors located on the surface of the cell. (3) In late endosomes/lysosomes (LE/lys) cholesteryl esters in LDLs are hydrolyzed to unesterified cholesterol, which is then distributed throughout the cell (4), to the plasma membrane via an unknown mechanism that requires NPC1. (5) as well as from the late endosomes/lysosomes to the endoplasmic reticulum (ER) where increased cholesterol content results in decreased synthesis of cholesterol and LDL receptors, and increased cholesterol esterification. Cholesterol that is synthesized in the ER is transported to the plasma membrane (6). In NPC1-deficient cells, unesterified cholesterol becomes sequestered in late endosomes/lysosomes so that the cholesterol content of the plasma membrane is reduced. Despite an overall accumulation of cholesterol in NPC1-deficient cells, the endoplasmic reticulum does not sense the increased cholesterol content in the cell and the synthesis of cholesterol and LDL receptors continues unregulated thereby resulting in cholesterol esterification that is inappropriately decreased.

Exogenously supplied LDL is endocytosed by the LDL receptor that is concentrated within clathrin-coated pits on the cell surface (Vance, 2006). Upon reaching the late endosomes/lysosomes, cholesteryl esters within the core of the LDL particles are hydrolyzed to unesterified cholesterol (Vance, 2006). Subsequently, in an NPC1-dependent pathway, the released cholesterol leaves the late endosomes/lysosomes and is distributed to other membranes including the plasma membrane and endoplasmic reticulum (Vance, 2006). Available data correlates with the idea that NPC1 and NPC2 both participate in the pathway for the egress of cholesterol from the late endosomes/lysosomes (Sleat et al., 2004b). The precise mechanism by which these proteins act in conjunction with one another remains elusive. Based on known motifs in the protein, and from functional studies on the mutant forms of NPC1, there have been several roles that have been proposed for NPC1 (Cruz et al., 2000; Davies et al., 2000; Ikonen and Holtta-Vuori, 2004; Mukherjee and Maxfield, 2004) including a cholesterol "flippase", a fatty acid permease, a ganglioside transporter, a cholesterol sensor that monitors the level of cholesterol in the lysosomal membrane and promotes the release of cholesterol from the membrane to an acceptor protein, and a member of a multi-protein complex that mediates cholesterol movement out of lysosomal membranes (Vance, 2006).

Recent studies suggest that NPC2 may function directly as a cholesterol transport protein (Cheruku et al., 2006). NPC2 is a soluble intra-lysosomal protein that has the capability of binding cholesterol. Storch et al. have shown in an *in vitro* transport assay that NPC2 transports cholesterol to phospholipid vesicles by way of a direct interaction with

acceptor membranes. This transfer is promoted by the addition of the lysosomal phospholipid, bis-monoacylglycerol phosphate, into the acceptor membranes (Cheruku et al., 2006). It is possible that NPC1 and NPC2 act together in a way where NPC1 acts as a sensor of cholesterol while NPC2 acts as the transporter. NPC2's presence in the lumen of the lysosomes/late endosomes allows it to function as an intralysosomal transport protein that shuttles cholesterol to the membrane bound NPC1 (Figure 7)

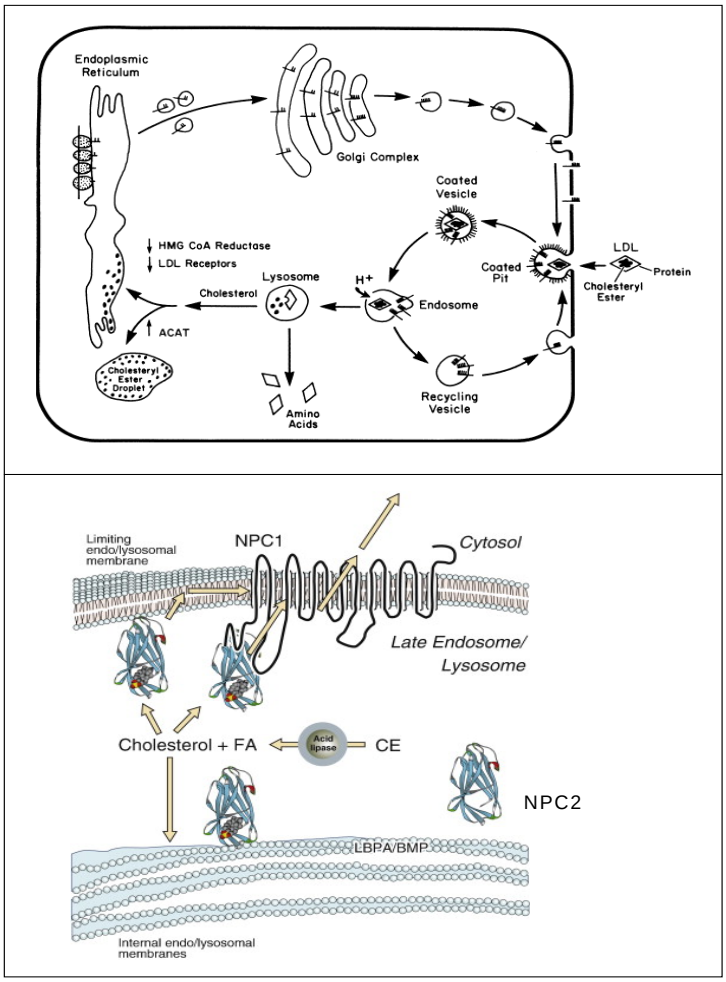

Figure 7: Top Panel from (Brown and Goldstein, 1985) The LDL receptor in mammalian cells. The receptor begins in the endoplasmic reticulum then travels to the Golgi complex, cell surface, coated pit, endosome, and then back to the surface. HMG CoA reductase denotes 3-hydroxy-3-methylglutary1 CoA reductase; ACAT denotes acyl-CoA: cholesterol acyltransferase. Vertical arrows indicate the direction of regulatory effects.) Bottom Panel from (Storch and Xu, 2009) Possible role of NPC2 in movement of cholesterol to NPC1 and out of the late endosomal/lysosomal compartment. CE, cholesteryl ester; FA, unesterified fatty acid; LBPA/BMP, lyso-bis phosphatidic acid, also known as bis(monoacylglycerol)phosphate.

9. NPC disease primarily affects the nervous system

It is presently unknown neurodegeneration results from an accumulation of cholesterol or gangliosides. Another question is whether the accumulation of cholesterol occurs as a result of ganglioside accumulation or vice versa (Puri et al., 2003; Puri et al., 1999; te Vruchte et al., 2004; Vanier, 1983; Zervas et al., 2001a). Also: are the characteristic neurological problems associated with NPC disease due to *excess* cholesterol in lysosomes/late endosomes or due to a *deficiency* of cholesterol at other cellular locations? The most prominent pathology of NPC disease is progressive loss of neurons, particularly of Purkinje cells in the cerebellum. Other significant characteristics of the disease are lipid storage disorders as well as formations of neurofibrillary tangles, meganeurites and ectopic dendrites (Walkley and Suzuki, 2004). Both the NPC1 and the NPC2 proteins are expressed in all tissues examined to date. This raises the question of why a loss of function of a ubiquitously expressed protein such as NPC2 would result in such devastating neurological pathology where neurons are particularly vulnerable.

The blood – brain barrier is impermeable to LDLs in the blood. The CNS has a lipoprotein transport system that is distinct from that exhibited in the plasma. In the CNS, cholesterol trafficking takes place through lipoproteins secreted by glial cells (primarily astrocytes). A parallel pathway is thought to operate in the peripheral nervous system whereby cholesterol is recovered from degenerating myelin and then delivered to neurons for growth and repair of axons. This re-utilization of cholesterol has been shown to be impaired in *Npc1* mice (Goodrum and Pentchev, 1997). It has been shown that induction of the NPC phenotype by treatment of cultured hippocampal neurons with a cholesterol

transport inhibitor, U18666A, decreases cholesterol content of axonal plasma membranes (Tashiro et al., 2004). This may imply that the defects seen in neuronal function may occur either because of lipid accumulation in the cell bodies or due to a deficiency of cholesterol in distal axons (Karten et al., 2002).

10. Potential avenues for therapeutic intervention in NPC disease

Thus far, there are no effective therapies for the treatment of NPC disease. One potential treatment for this disease is that of gene therapy where the wild-type NPC2 gene would be delivered to patients with a defective form of the gene thereby resulting in the restoration of function. Again, the blood-brain barrier obstacle would have to be overcome for this to be most effective. This can be done by delivering therapeutic agents directly to the CNS or by using therapeutic substances that can readily cross this barrier. In NPC1 and NPC2 deficient mice, there is an accumulation of cholesterol and gangliosides in late endosomes/lysosomes. Due to this phenomenon, there have been initial attempts for finding a treatment for NPC that focus on methods that would reduce the levels of cholesterol and other material in tissues, mainly brain. Such attempts include the introduction of a null mutation in the LDL receptor into Npc1 -/- mice. This was shown to partially reduce the storage of cholesterol but did not improve the resultant neurological symptoms of this disease (Erickson et al., 2000). Agents that lower plasma cholesterol and other dietary measures have been unsuccessful in slowing the neurological progression of this disease (Patterson and Platt, 2004). Due to the vast accumulation of gangliosides in tissues of both NPC1-deficient humans as well as mice, there have been suggestions for a strategy, which would reduce the amounts of these lipids in the brain. This led to the Npc1 -/- mice being crossed with mice that where null for N-acetylgalactosamine transferase. These double knockout mice were unable to synthesize the GM2 ganglioside and still, their life span was unaffected. These results suggest that the accumulation of GM2 is not what causes the disease state in mice. Npc1

-/- mice were also given N-butyldeoxynojirimycin which is a potent inhibitor of the first step in synthesis of all glycosphingolipids, including gangliosides (Vance, 2006). The lifespan of these mice was extended by about 20% and some neurological symptoms were delayed (Zervas et al., 2001b). As a result of these findings, there are now clinical trials that are being performed on children with NPC disease using this inhibitor (Vance, 2006). Another promising approach for treatment of this disease arises from studies of the levels of neurosteroids which were found to be significantly reduced in the brains of NPC1 deficient mice, particularly in the cerebellum (Griffin et al., 2004). When one of these neurosteroids, allopregnalone, was administered to neonatal Npc1 -/- mice, the median survival was increased from 67 days to 124days (Griffin et al., 2004) suggesting that neurosteroid treatment of NPC disease may be beneficial. However, more recent work indicates that the carrier used to deliver the neurosteroids, cyclodextrin, was as effective as neurosteroids alone (Liu et al., 2009).

11. The NPC mouse models

11a. *Npc1* Mouse

Understanding the molecular basis of Niemann-Pick C (NPC) disease was a daunting and arduous task that took decades of hard work by many scientists. Due to the fact that the NPC disease was grouped as an Niemann-Pick disorder, there was a considerable amount of time and effort spent on looking for clues that proved that this disease, like NPA and NPB, had a defect in lysosomal sphingomyelinase activity (Brady et al., 1966). It was only after the collective collaborations of many scientists that they were able to begin unraveling the complex lipid-storage mystery that was observed in the NPC tissues. Further studies were aided considerably with the discovery of a spontaneous mouse mutant for *Npc1*. Because of this mouse, researchers were pointed down the right path towards characterization of this disease and towards distinguishing it as genetically distinct from Gaucher disease. In these NPC1 mutant mice, all hepatic cholesterol stored was unesterified (Pentchev, 2004). In an experiment where mice underwent five weeks of cholesterol feeding, scientists were stunned by the enormous pale white livers found in these mutant mice. The lipid measurements they then performed revealed that, unlike normal mice, all cholesterol derived from the diet was in the form of free unesterified cholesterol and not cholesteryl esters (Pentchev et al., 1984). The same result was seen in mutant mice fibroblasts. These findings represented the first critical link between NPC disease and cholesterol metabolism, more specifically, a defective LDL-stimulated cholesterol esterification (Pentchev, 2004). After it was established that this mouse mutant is a model for the NPC1 disease, Carstea identified the gene in humans using

positional cloning (Carstea et al., 1997). Positional cloning allows for the identification of genes without having first identified the protein. At a later date, Sleat et al used the *Npc1* knockout mouse to cross with the *Npc2* hypomorph generated in our lab so that studies can be done to elucidate how NPC1 and NPC2 might interact with one another in lipid transport (Sleat et al., 2004b).

11b. *Npc2* mouse

In order to gain insight into the function of NPC2 and how it may interact with NPC1, we targeted the murine gene and generated a severe hypomorph expressing between 0-4 % residual protein in different tissues (Sleat et al., 2004b). The phenotype of this hypomorph was then studied in the presence and absence of *Npc1*. Week 9.5 129 SvEv embryonic stem cells (ES cells), from Colin Stewart (National Cancer Institute, Frederick, MD), were electroporated using a Bio-Rad gene Pulser with vector DNA that was linearized with *Not*I and targeted clones were selected by using neomycin and gancyclovir. Screening was then performed by Southern blotting by using a probe that detected a 4.1 kb *Bgl*II product that was specific to the targeted allele (Figure. 6 from (Sleat et al., 2004b). The targeted ES cell clone was then identified, expanded, and used for microinjection. The ES cells were injected into C57BL6 blastocysts that were then transferred in pseudo pregnant Swiss-Webster females (Sleat et al., 2004b). The highly chimeric males were then used to mate with C57BL6 females and a number of offspring were generated and confirmed to be heterozygous for the *Npc2* gene by Southern blotting (Sleat et al., 2004b). An aberrant recombination event took place in these mice resulting

in the insertion of the neo selection marker and part of the left arm containing intron 1 and intron 2. These lead to the requirement of having two separate PCR reactions in order to differentiate between the heterozygous and homozygous targeted mice (Sleat et al., 2004b). In this *Npc2* –targeted mouse, correctly spliced mRNA was present at greatly reduced amounts compared to the wild-type mouse (Sleat et al., 2004b) 2.1% in brain and 4.5% in epididymis as shown by real-time PCR and quantitative immunodetection revealed only 3.5 ± 0.9% of normal NPC2 protein levels in epididymis with little or no expression in most other tissues examined (Sleat et al., 2004b).

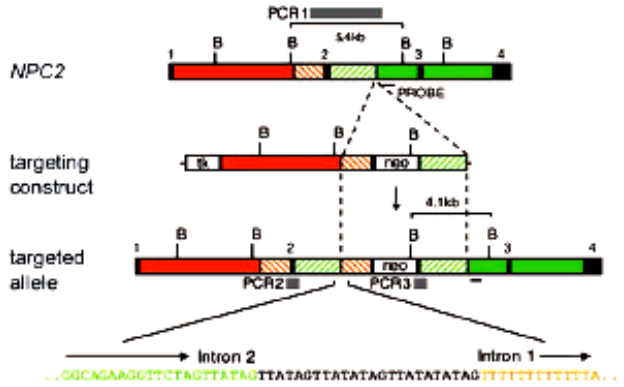

Figure. 8: From (Sleat et al., 2004b)Targeted disruption of the murine NPC2 gene (*NPC2*). Structure of *NPC2*, the targeting construct, the targeted locus and the sequence at the *NPC2* intron 2:left arm intron 1 junction. *Bgl*II sites; boxes: black shading, exons; unshaded, thymidine kinase (tk) and neo; orange, intron 1; green, introns 2 and 3; green and orange dashed, sequences duplicated in the targeted allele. The strategy for inactivating *NPC2* was to insert a loxP-flanked neo cassette into exon 2 with the concomitant replacement of amino acid cysteine 42 with a stop codon and a deletion of amino acids 43–53.Anaberrant recombination event, characterized by Southern blotting and sequencing of genomic PCR products, resulted in the insertion of the neo selection marker and part of the left arm containing intron 1 into intron 2 of *NPC2*. Twenty-four nucleotides of unknown derivation are inserted at the site of the intron 2 – intron 1 junction. Gray bars depict informative PCR products PCR1, PCR2, and PCR3 for NPC2 genotyping.

The experimental data collectively indicates that the *Npc2*-targeted mouse is a severe hypomorph rather than a null. This is consistent with the gene disruption of exon 2 where aberrant recombination resulted in the insertion of the neo selection marker and part of the left arm containing intron 1 into intron 2 (Figure. 8 from (Sleat et al., 2004b). The *Npc2* hypomorph was relatively normal until approximately 55 days where weights began to drop rapidly until the time of death due to disease, or euthanasia due to morbidity see Figure. 9A from (Sleat et al., 2004b).

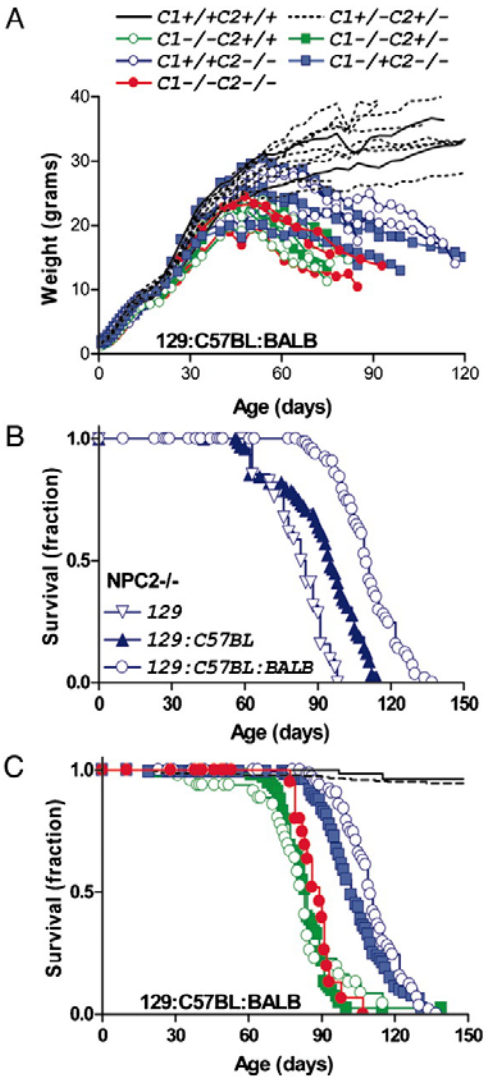

Figure. 9: From (Sleat et al., 2004b) Growth and survival of NPC2 hypomorph mice in the presence or absence of NPC1. (A) Growth of male NPC mutant mice. (B) Survival of NPC2 hypomorph mice in different genetic backgrounds. (C) Survival of NPC2 hypomorph mice in the presence or absence of NPC1. Symbols are as in A; control, n = 11 (two NPC1+/+;NPC2+/+, nine NPC1+/–;NPC2+/–); NPC1 mutant n = 7 (five NPC1–/–;NPC2+/– and two NPC1+/+); NPC2 mutant n = 6 (three NPC1+/+;NPC2–/– and three NPC1+/–;NPC2–/–) and NPC1-NPC2 double mutant, n = 3.

A continuous tremor was detected at around 55 days and was eventually accompanied by ataxia and total locomotor dysfunction (Sleat et al., 2004b). These mice expired between 90 and 130 days of age. This was influenced by genetic background of the mice perhaps due to strain-specific modifiers as had been proposed for *Npc1* mouse mutants (Miyawaki et al., 1986; Sleat et al., 2004b; Zhang and Erickson, 2000). The onset of disease in this hypomorphic mouse model was later in progression and less rapid when compared to the *Npc1* mutants of similar genetic background (Figure. 9B from (Sleat et al., 2004b)). This probably reflects that these mice are severe hypomorphs rather than null mutants. Double mutant mice are indistinguishable from the single *Npc1* mutant in terms of gross neurological symptoms as well as time of disease onset and progression see above two Figures 9A and 9C (Sleat et al., 2004b). The reasoning behind the investigation of how the NPC1 and NPC2 proteins interact was to help better understand whether these two proteins play an independent role in lipid transport. If their molecular roles were in fact unrelated, then a more severe phenotype than either of the individual mutant mouse phenotypes might be expected when both the *Npc1* and *Npc2* mutant mice were crossed (Sleat et al., 2004b). In contrast to this hypothesis, one would expect that if the phenotypes were the same, or relatively close in nature, that the *Npc1/Npc2* double mutant mouse may act in a cooperative function in lipid transport. We showed that in fact, the phenotypes of the *Npc1*, when compared to that of the *Npc1/Npc2* double mutant, appear to be indistinguishable. Furthermore, the phenotype of the *Npc2* mouse is very similar but with a slightly later onset and slower progression of disease (Sleat et al., 2004b). The cross between the *Npc1* and *Npc2* mice provided great genetic evidence for a cellular pathway for the transport of lysosomal lipids where both proteins participate and

where neither protein can compensate for the loss of the other (Sleat et al., 2004b). The roles of each protein in a specific pathway and their function or physical interactions have yet to be determined. It may be that NPC2 is involved in the transportation of free cholesterol through the aqueous lumen of the late endosome/lysosome to the membrane where NPC1 might detect changes in cholesterol levels thereby consequently regulating the movement of lipids within the lumen by either altering vesicular transport or by participating directly in cholesterol transfer across the membrane (Sleat et al., 2004b). The *Npc1* -/- mouse along with the *Npc2* hypomorph will allow for experimentation utilizing many different approaches for the verification of these hypotheses. In addition to providing a useful system for investigating the function of the NPC pathway, the mouse models also provide a system for preclinical studies of potential therapeutics. Finally, one can use the mutant mice as negative controls to evaluate the specificity of immunodetection procedures for NPC1 and NPC2.

12. Rationale

A valuable method used in studying a genetic disease in humans is through the use of targeted gene mutation, a powerful technology that has revolutionized biomedical research (Crawley, 2000). A disease that is inherited genetically in humans is pinpointed to a chromosomal locus and the gene is then identified by mapping. A DNA construct containing the mutated form of the gene is then developed and inserted into the mouse genome. A colony of mice with this mutation is generated and characteristics of these mice are then identified in comparison to normal controls. Characteristics of these models that resemble those in the human disease are evaluated and then used to test the effectiveness of treatments (Crawley, 2000). Genetically altered mice can provide excellent models of human physiology and disease and allow for the evaluation of the effect of a single altered gene in the context of the whole organism. This can provide tremendous insights into gene function. The mouse model provides an excellent tool for investigation of molecular mechanisms underlying lysosomal diseases such as cLINCL, NPC1 and NPC2 and the resulting devastating disorders that affect the largely inaccessible tissues of the central nervous system. These models enable us to assess behavioral, pathological, cellular, and molecular abnormalities and allow for the development of novel therapies for these thus far incurable diseases.

Characterization of our mouse models for these lysosomal diseases provides us with insight into the etiology of the human disease as well as allows us to test putative treatments on mice before going to clinical trials. Many of the characteristics of these

diseases in humans are mimicked in our mice and an improvement in these models is likely to translate into an improvement in affected patients. In mice, this can be tested by way of survival curves and other behavioral methods that allow us to test for the improvement or decline in neurological symptoms that are a characteristic of these lysosomal diseases. Such behavioral methods include rota-rod and gait analysis experiments among others as described previously in (Sleat et al., 2008; Sleat et al., 2004a; Sleat et al., 2004b). The *Cln2* hypomorph mouse model provides us with an estimate of the TPP1 levels needed for successful treatment of this disease as well as enlightens us with the necessary starting point for further studies using various therapeutic approaches. The CLN2 and NPC mice can be used in various studies such as chemical chaperone therapy, enzyme replacement therapy, neural stem cell therapy, gene therapy, convection-enhanced delivery of proteins and hematopoietic stem cell therapy (cord blood transplant). In the previous section, I have given background on LINCL and NPC disease and have described published work. These include my contributions towards generating and characterizing the TPP1-deficient and NPC-deficient mouse models, where my role was to do the majority of the live animal analysis (genotype animals, conduct backcrosses, collect weight and survival data, perform behavioral analysis) and to help with other aspects of the project. This work is described in the following papers,(Sleat et al., 2008; Sleat et al., 2004a; Sleat et al., 2004b).

The study of lysosomal storage disorders such as cLINCL and NPC disease and their effects on the nervous system, particularly the brain, require an approach that allows for the characterization of the localization of the molecules involved while they are in their

morphological context. Key for understanding the biological function of these proteins is understanding their cellular localization. This may aid in the identification of molecular mechanisms involved in the neurodegeneration seen in these diseases. A detailed description of the methods used in the immunohistochemical study of protein localization using our mouse models of lysosomal storage disorders will provide a solid footing for future studies to come and will allow for consistent and optimal morphological preservation, reproducibility and quantitative assessment especially when evaluating the effects of protein or enzyme supplementation in our knockout models for cLINCL and NPC disease. In the remainder of this thesis I will describe mostly unpublished work towards developing immunohistochemical methods to detect TPP1, NPC1, and NPC2 in mouse tissues. The TPP1 procedure was successful and has been implemented as a routine protocol in our laboratory for different projects including the published characterization of the hypomorphic TPP1 model (Sleat et al., 2008). The NPC proteins were more problematic but I will discuss various procedures that I used in an attempt to obtain a specific immunodetection protocol. The core techniques used in this study and the rationale behind using them will be explained in the following sections.

12a. Overview of Immunohistochemistry

Immunohistochemistry (IHC) refers to the process of localizing proteins in cells of a tissue section by exploiting the principle of antibodies binding specifically to antigens in biological tissues (Ramos-Vara, 2005). IHC is a method that is widely used in research to aid in understanding the distribution and specificity of localization of proteins in different parts of a tissue. This portion of my thesis will cover technical aspects of IHC involving our mouse models of lysosomal disease and the best protocols for use in visualizing the antigen/antibody complexes that are crucial for our ongoing studies. Procedures involving testing fixatives for initial fixation followed by methods of post-fixation, cryo-sectioning of tissue, antigen retrieval using cryo-sections, different detection systems of antibody using direct and indirect methods and finally, troubleshooting and the optimization of signal to noise ratio for faster and more reliable interpretation of results will all be discussed, in detail, in the subsequent sections. The overall procedure involved can be visualized in the following flow-chart Figure 10.

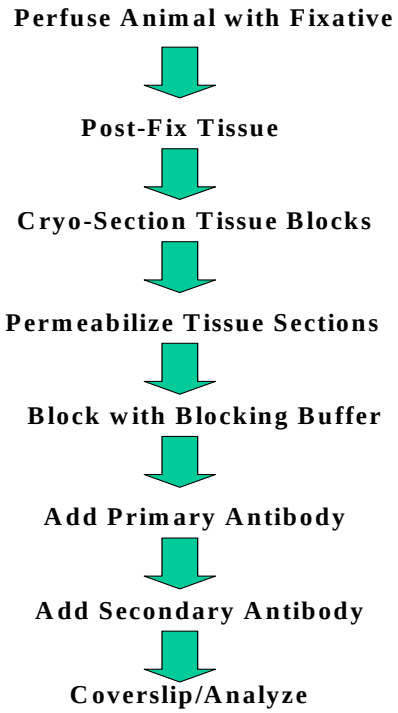

Figure 10: Summary process used for Immunohistochemical detection of Antibody/Antigen complex between antibodies and proteins of interest

12b. Intracardiac Perfusion

Intracardiac perfusion allows for tissues to be fixed in situ (the tissue does not die until it is fixed) and at a rapid rate so that tissues are preserved quickly to prevent degradation of proteins and tissue. For intracardiac perfusion, a surgical depth of anesthesia is attained where the mouse does not respond when its foot is firmly pinched. This is achieved by injecting the mouse intraperitoneally with a 1:4 dilution of euthanasia solution, Euthasol, a mixture of 390 mg pentobarbital sodium (barbituric acid derivative), 50 mg phenytoin sodium (Virbac Animal Health, Fort Worth, TX) and distilled H_2O. The chest around the sternum is opened and a cut is made in the right atrium of the mouse heart. A needle is

placed in the left ventricle of the mouse heart and 20-50ml of PBS at pH7.4 at a speed of 18ml/min, is flushed through the heart until the liver is clear from blood. This is an indication that most of the blood has been flushed out of the animal and therefore will be less likely to interfere with subsequent steps. Thereafter, 50-100ml of fixative is flushed in at the same speed until the body becomes stiff. This is an indication that the whole body of the animal has been successfully perfused with fixative. Tissues are then collected and drop fixed in 4% paraformaldehyde (PFA) (Electron Microscopy Sciences, Hatfield, PA) or Bouins reagent. We have found that intracardiac perfusion is the most effective fixation method because it allows for complete and even distribution of fixative throughout all tissues. This method works to fix tissues from the inside out by way of the circulatory system. Fixation by intracardiac perfusion is recommended for tissues that autolyse rapidly, such as nervous tissue or endocrine tissue. For some studies, perfusion is not possible, and an immersion fixation or "drop fix" can be acceptable for certain types of stains, however, for our studies, we have found that intracardiac perfusion by flushing with 1x PBS followed by intracardiac perfusion using Bouins fixative (Electron Microscopy Sciences, Hatfield, PA) yields the best results when looking at the distribution of TPP1 and NPC2 proteins, while perfusion with 4% PFA worked best for NPC1.

12c. Fixative/post-fixative

Major factors in determining how easy an antigen is to detect are the characteristic of the antibodies and the type of fixative being used. Living cells and tissues are dynamic in nature and most cell staining methods require that cells be fixed. Perfect fixation would immobilize the antigens while preserving cellular and subcellular morphology and at the same time would permit easy access of antibodies to cells and subcellular structures. The fixative functions as a cross-linking reagent that helps to preserve the tissue as close to its natural state as possible by acting to prevent against intrinsic bio-molecules (proteo-lytic enzymes that would digest or damage tissue) as well as extrinsic damage due to microorganisms (bacteria). There is no perfect fixation method, however one could optimize conditions so that the best results could be attained. The selection of fixative depends on the eventual procedure to be used, as described below. Fixation times are mainly a function of sample size and adult organs are normally fixed overnight at 4ºC (Franco et al., 2001). Both under-fixation and over-fixation might result in ectopic staining, high background level or no staining at all (Franco et al., 2001). Under-fixation may result in loss of proteins (antigen) and decreased preservation of tissue and over-fixation results in the antibody not being able to perfuse into the tissue and recognize the antigen. Thus, one of the key steps in successful protein detection is the selection of both the optimal perfused fixative and post-fixative necessary for the antibody. There are labs who have benefited from the use of a post-fixation using methanol/acetone/water (MAW) for the localization of proteins by way of indirect IHC on tissue sections (Franco et al., 2001). They found that this fix worked when they experienced weak or no staining with

more conventional fixatives such as formaline, formaldehyde and Bouins reagent. Another advantage of MAW as a fixative is that it combines a good preservation of the morphology and immunogenicty because it works as a precipitating rather than a cross-linking fixative. The use of MAW as a post-fixative also provided excellent results with antibodies used with tissues that were previously formaldehyde-fixed. They also found that formaldehyde, a cross-linking fixative, might be beneficial for the detection of membrane-bound proteins (Franco et al., 2001). Since NPC1 is a membrane protein, we chose to evaluate this as a fixative as well. .

CLN2

To investigate post fixation for the lysosomal protein TPP1 in mouse brain, a series of intracardiac perfused fixes were paired with a series of post-fix conditions. Results were analyzed for staining conditions that resulted in the most specific binding of the antibody with the least background. These conditions are described in Table 2 below. These experiments were conducted using the CLN2 mouse and α-TPP1 antibody R72-5 which was produced and characterized in our lab, using a recombinant human CLN2 protein as an immunogen (Lin et al., 2001). Both MAW and Histochoice MB, a 40% glyoxal, sodium chloride and ethanol mixture, (Electron Microscopy Sciences, Hatfield, PA) were used as mild post-fixation conditions to help us analyze whether a milder post-fix would improve antigen/antibody binding.

NPC

For the evaluation of conditions for the NPC proteins in mouse brain, it was necessary to test out what fixative and post-fixation combination, would best suit our needs for detecting the lysosomal proteins NPC1 and NPC2. For this, a series of intracardiac perfused fixes were paired with a series of post-fix conditions, and results were analyzed for best staining results. This was done with the hope that we would be able to develop a protocol that would enable us to visualize both NPC1 and NPC2 proteins simultaneously. This was done using the NPC1 and NPC2 mouse models and a number of corresponding antibodies in search of the antibody which will give us the strongest signal with the least noise (background).The best results were realized with the antibodies, rabbit polyclonal anti Niemann-Pick C1 (Novus Biologicals) and the affinity purified α-NPC2 antibody HL5873, an antibody generated in our laboratory by immunizing rabbits with recombinant human NPC2 produced in Chinese Hamster Ovary Cells) (Table 3). When analyzing post-fixation conditions for each antibody, it was found that a post-fix that worked well with one antibody, impacted negatively on the other (see Figures 12-13). These results stand in the way of our ultimate goal of looking at both lysosomal NPC proteins concurrently and therefore this idea was abandoned in the final protocol.

PERFUSION FIX	POST-FIX	POST-FIX TIME
4% PFA in 0.1M PBS @ rate of 18ml/min	Histochoice	O/N
	MAW	O/N
	4% PFA	2 Hrs
	4% PFA	4 Hrs
	4% PFA	O/N
	Bouins	3Hrs
Bouins @ rate of 18ml/min	Bouins	3Hrs
	Bouins	O/N
	Histochoice	O/N
	MAW	O/N

Table 2: Perfusion fix and corresponding post-fix conditions used in evaluation of best fixative conditions for use in staining of TPP1, NPC1 and NPC2 lysosomal proteins in mouse brain. Abbreviations are: Paraformaldehyde (PFA), Methanol/Acetone/Water (MAW), Overnight (O/N)

12d. Preparation of tissues for cryo-sectioning

Although fixation and post-fixation are both very important in their effects on the antigen/antibody reaction, tissue processing may have an additional effect on the preservation of antigenicity. The combination of cross-linking fixatives with heat and nonpolar solvents that are used during the process of paraffin embedding frequently modifies the conformation of antigens resulting in an inability of specific epitopes to be recognized by antibodies that have been previously been recognized using frozen sections (Ramos-Vara, 2005). While cryosectioning requires more effort and care, we chose this route in the interest of preserving immunoreactivity.

Embedding tissues for use in cryo-stat sectioning is carried out by first rinsing with 3 consecutive washes of 1x PBS to clear the post-fix followed by immersion of the tissues in 15% Sucrose in PBS and then 30% Sucrose in PBS. This step equilibrates the tissue

with embedding medium, allowing for a solid flat sheet of tissue surrounded by the medium to be evenly cut when cryo-stat sections are prepared. Our lab utilizes both Tissue-Tek Optimal Cutting Temperature Compound (OCT) Compound (Sakura Finetek USA, Inc., Torrance, CA) .The embedding matrix allows for easier tissue manipulation and cutting at low temperature required for preparing cryo-sections as well as prevents the formation of harmful ice crystals forming on and damaging the tissue specimen. The OCT embedding matrix is mostly comprised of polyvinyl alcohol and polyethelene glycol and is aqueous in nature to prevent an accumulation of residue on tissue specimens, which may lead to undesirable background staining. A plastic disposable embedding mold was used for freezing the tissue into blocks. A small amount of embedding media is first added to cover the bottom. The tissue is then placed in the correct orientation required for sectioning and then covered completely with embedding medium. The mold is then placed in a 2-methylbutane bath on dry ice for freeze-down before transferring to –80˚C for storage.

12e. Cryo-stat sectioning/slide preparation

Tissue blocks are moved into the cryo-stat for at least 30 minutes so that they were equilibrated to the desirable cutting temperature at -17 to -20˚C. Superfrost plus slides (Fisher Scientific, Pittsburgh, PA) coated with TESPA (3-aminopropyl-triethoxysilane) were used for optimum tissue adherence. A drop of 1xPBS at pH 7.5 was added to the slide before touching the slide to the freshly cut section. This allowed for even spreading of the section with less folding than observed when very thin sections (10µm) were cut.

The Leica CM1900 (Leica Microsystems, Wetzlar, Germany) was used to cut three sequential tissue sections per slide. Slides were kept in the laboratory at room temperature overnight for drying to achieve maximal tissue to slide adherence. This is especially important when working with cryo-sections because it helps in preventing any tissue loss during subsequent washes and staining. Slides were either used the next day or stored at -80˚C in a slide box with a dessicator to avoid condensation and the formation of any harmful ice crystals on the sections.

12f. Tissue antibody staining procedures

Frozen slides were thawed at 4˚C for 1 hr to overnight or, if going to be used immediately, at room temperature for 20 minutes or as long as it takes for condensation to be eliminated and for the slide to be dry. If sections on the slide are going to be treated individually, a PAP pen (Electron Microscopy Science, Hatfield, PA) hydrophobic slide marker is used to draw a circle around each tissue section. Once this has dried, the slides are subjected to three consecutive washes in 1x PBS for 5 minutes each to remove any residual fixative. Slides are then permeabilized using 0.5% TritonX100 in PBS for 10 minutes. This step permeabilizes the plasma membrane as well as the membranes of internal organelles so that the antibody has access to intracellular proteins. Following permeabilization, a specific blocking buffer was used, depending on the primary antibody used. If a standard 3% BSA (Bovine serum albumin) in PBS/0.2% Tween 20 block was insufficient for preventing non-specific background staining, an alternative block was used. The optimal blocking buffer was chosen based on extensive trials where the results

were evaluated in terms of signal to noise. Results are shown in Table 2. In previous studies using the TPP1 antibody, a blocking buffer with a higher salt concentration, 500mM NaCl, alleviated high background noise (Lin et al., 2001). The reduction of non-specific background staining due to ionic interactions has been shown to be alleviated by increasing salt concentration (NaCl or KCl) in the buffer to 0.5M (Ramos-Vara, 2005). This increase in ionic strength can also disrupt the binding of specific but low affinity binding and should therefore be used only when necessary to reduce high levels of background so that the true signal can be seen more clearly (Ramos-Vara, 2005). All blocking was done for 30 minutes as shown in Table 4.

After blocking was complete, the primary antibody was added at varying dilutions for optimization of signal to noise ratio. A series of candidate antibodies were tested at various dilutions for each protein of interest (Table 3).

PROTEIN	ANTIBODY TESTED	SIGNAL	SPECIFICITY	DILUTION
TPP1	Anti-TPPI R72-5	+++	++	1:100,1:300, 1:600
NPC1	Santa Cruz NPC1(C-21): sc-18201	NONE	N/A	1:50
	MS59 rabbit antibody against Loop A	NONE	N/A	1:100,1:250, 1:400,1:500, 1:5000
	MS45 rabbit antibody against NPC1 Internal Loop	+++	NONE	1:250, 1:500,1:750, 1:1000
	Rabbit Antibody against Cytoplasmic Tail	NONE	N/A	1:100,1:250, 1:400,1:500, 1:5000
	Novus Biologicals rabbit polyclonal anti Niemann-Pick C1	+++	++	1:250, 1:500,1:750, 1:1000
NPC2	Affinity Purified HL5873	+++	++	1:100, 1:500, 1:1000
	Affinity Purified HL5874	++	++	1:100, 1:500, 1:1000
	Affinity Purified HL5895	++	NONE	1:100, 1:500, 1:1000

Table 3: Candidate antibodies were tested for signal strength and specificity. This was done using wild-type mouse brain sections to depict a positive signal and knockout mouse brain sections as a control. In the knockout mouse, there should be no signal present allowing for a way to measure specificity of the antibody to the antigen. Antibodies highlighted in yellow represent the final chosen antibodies.

These experiments allowed us to narrow down possible antibody candidates for use in further optimization studies. The chosen antibodies are highlighted above in (Table 3). One criteria for antibody choice was the specificity of signal. This was done by

comparing side by side staining of wild-type mouse brain sections, where staining should be present, and knock-out mouse brain sections, where no staining should be present. With some of the antibodies, there was some non-specific staining present, however, the amount of specific staining was significantly higher when compared to knockout mouse brain sections.

12g. Methods for Improving Signal: Noise Ratio

Nonspecific antibody binding is one of the main causes of perplexing background staining in IHC (Rogers et al., 2006). For the chosen antibodies, different blocking buffers were used, as shown below in (Table 4), with the aim being to increase specificity without compromising signal strength.

1˚ Ab	BLOCKING BUFFER	NOISE	SIGNAL	BLOCK TIME
TPP1	3%BSA/PBS/0.2%Tween20	+++	+++	30 min
	3%BSA/500mMNaCl/PBS/ 0.2% Tween20	+	++	30 min
NPC1	3%BSA/PBS/0.2%Tween20	+++	+++	30 min
	3%BSA/500mMNaCl/PBS/ 0.2% Tween20	++	+++	30 min
	3%BSA/500mMKCl/PBS/ 0.2% Tween20	+	+++	30 min
NPC2	3%BSA/PBS/0.2%Tween20	+++	+++	30 min
	3%BSA/500mMNaCl/PBS/ 0.2% Tween20	+++	++	30 min
	3%BSA/500mMKCl/PBS/ 0.2% Tween20	+	++	30 min

Table 4: Several blocking buffers were used in the optimization of the signal to noise ratio for each antibody. Comparative results are indicated by a + where +++ is high background, + + is lower background and a + is lowest background.

There are other methods, which can be used to prevent non-specific binding of antibodies. It is possible that background staining may be due to the spontaneous reduction of immunoglobulin disulfide bonds and that non-specific antibody binding in IHC can be mediated by sulfhydryl interactions (Rogers et al., 2006). For this reason, in addition to varying the type of blocking buffer used, the reduced form of glutathione (GSH) can be co-incubated with the primary antibody in pH 8 tris-EDTA (TE) buffer. GSH in concentrations ranging from 30-90μM have previously been shown to prevent nonspecific background in frozen and ethanol-fixed sections (Rogers et al., 2006). GSH supplementation was tested using the Novus Biologicals NPC1 antibody and HL5873 and

HL5874 NPC2 antibodies and the signal: noise ratio was analyzed. The lowest effective (30μM concentration) was used for an initial test as to whether GSH supplementation would be effective for reduction of background staining. Analysis of mouse brain sections of wild-type vs. knock-out showed a significant reduction in both signal and noise. The lowest suggested concentration proved not to be helpful, even though multiple antibody dilutions were used (Table 5), so no other concentration of GSH was tested.

PRIMARY ANTIBODY	ANTIBODY CONCENTRATION	SIGNAL	NOISE	GSH (μM)
NPC1-Novus Biologicals	1:100	+	-	30
	1:250	-	-	30
	1:500	-	-	30
NPC2 HL5873	1:100	+	-	30
	1:500	-	-	30
NPC2 HL5874	1:100	+	-	30
	1:500	-	-	30

Table 5: The use of GSH in signal: noise optimization. GSH shown to dramatically weaken overall signal at various concentrations of primary antibody. Comparative results are indicated by a (+) where +++ is high signal, + + is lower signal and a + is lowest signal. A (-) denotes no signal or noise (background).

Another method for improving signal: noise ratio in cryostat frozen tissue sections is through the use of 1% Sodium Dodecyl Sulfate (SDS) in PBS (Brown et al., 1996). This is a type of antigen retrieval method that allows for more antigens to be uncovered so that the primary antibody is able to access binding sites more readily. This method was employed before blocking and slides were treated with this solution for 5 minutes at room temperature. Comparison between slides treated with SDS and slides that were not revealed no significant difference in strength of signal or reduction of noise.

A final method used to reduce background is that of Heat Induced Epitope Retrieval (HIER). Antigen retrieval is more widely used on paraffin embedded sections, however, there have been studies that report that antigen retrieval using fixed frozen sections has been used successfully in enhancing immunoreactivity and effectively lowering background staining (Ino, 2003). This step was added into the protocol before permeabilization of the slides. Glass staining slide chambers were filled with Antigen Unmasking Solution (Citrate Salt Based) H-3300 (Vector Laboratories, Inc., Burlingame, CA) and microwaved until boiling. Slides were inserted into the boiled solution for 30 minutes and then processed according to protocol. Analysis of these slides revealed that HIER improved the signal for the antibodies by significantly increasing staining specificity but may also result in increased background staining.

12h. Detection/Secondary Antibody

Detection or visualization of the antigen/antibody complex can be accomplished in a number of ways. In some instances, the antibody can be conjugated to an enzyme, such as peroxidase, which can catalyze a color producing reaction. In other instances, the antibody can be tagged to a fluorescent fluorophore such as FITC, rhodamine, Texas Red, Alexa Fluor, or DyLight Fluor. The fluorophore method is of great use in confocal laser scanning microscopy, a highly sensitive technique that can also be used to visualize interactions between multiple proteins. With the appropriate fluorescent antibodies, it is possible to look at more than one antigen using different fluorophores. For this reason, we chose to optimize the use of this method of detection using the Alexa Fluor 488 goat anti-rabbit IgG (Invitrogen) at their recommended dilution of 1:400. For the detection of

the antigen: antibody complex, a laser-scanning confocal microscope, the Zeiss LSM-410, was used because of its ability to slice clean thin optical sections out of thick tissue specimens. To observe organelles, we used a high power 63x oil objective.. We used a biotinylated, soluble form of the cation-independent mannose 6-phosphate receptor (sCI-MPR) as a marker of brain lysosomes, (This recognizes the mannose 6-phosphate recognition marker used to target lysosomal proteins to the lysosome, and this marker is largely retained in neuronal lysosomes). The secondary antibody for this was a steptavidin conjugated antibody which when bound to the biotin on the sCI-MPR, fluoresces red (555nm). If in fact the antibodies against the proteins do co-localize within the lysosome, they will appear yellow in color when the images are merged. This allowed us to test whether or not the signal for our protein was within the lysosome. If similar conditions are needed for both NPC1 and NPC2, then the localization of these proteins could be further studied within the mouse brain. Since both of these antibodies are from the same species, it could be very problematic trying to distinguish between these two proteins. One way of solving this problem is by obtaining an antibody against either NPC1 or NPC2 that was raised in a different species so that it would be possible to look at both proteins at the same time. An example would be having the NPC2 raised in donkey and then having a different wavelength fluorophore against donkey IgG. This would allow for us to look at how both proteins co-localize throughout the mouse brain by merging the pictures taken of each antibody's expression using the confocal microscope.

13. Analysis/Conclusions

Targeted gene mutation in mice represents a powerful technology that revolutionized biomedical research. The mouse model provides an excellent tool for investigation of molecular mechanisms underlying lysosomal diseases such as cLINCL, NPC1 and NPC2 and the resulting devastating disorders that affect the largely inaccessible tissues of the central nervous system. These models enable us to assess behavioral, pathological, cellular, and molecular abnormalities and allow for the development of novel therapies for these thus far incurable diseases.

Characterization of our mouse models for these lysosomal diseases provides us with insight into the etiology of the human disease as well as allows us to test putative treatments on mice before going to clinical trials. Many of the characteristics of these diseases in humans are mimicked in our mice. Therefore, if improvement is seen in the disease in these models, it is likely that improvements could be possible in patients. In mice, this can be tested by way of survival curves and other behavioral methods that allow us to test for the improvement or decline in neurological symptoms that are a characteristic of these lysosomal diseases. Such behavioral methods include rota-rod and gait analysis experiments among others. The *Cln2* hypomorph mouse model provides us with an estimate of the TPP1 levels necessary for successful treatment of this disease as well as enlightens us with the necessary starting point for further studies using various therapeutic approaches. The CLN2 and NPC mice can be used in various studies such as chemical chaperone therapy, enzyme replacement therapy, neural stem cell therapy, gene

therapy, convection-enhanced delivery of proteins and hematopoietic stem cell therapy (cord blood transplant).

Investigation of lysosomal storage disorders such as cLINCL and NPC can be realized through the utilization of immunohistochemistry using mouse models in order to aid in elucidating the specific localization of proteins associated with these diseases. This is especially important when looking at protein distributions within the brain following treatment with any potential therapeutic protein or enzyme such as those used in protein or enzyme replacement therapies (TPP1) or when looking to study the localization/co-localization of the proteins (NPC 1 and 2). In this laboratory, we have become progressively experienced in determining the best possible methods for detecting these proteins using cryo-preserved tissues and immunohistochemistry.

Analysis of final figures (Figures 11-13), illustrating how well the antigen: antibody complex could be visualized, revealed the optimum conditions for each antibody (TPP1, NPC1 and NPC2).

The TPP1 antibody was successfully visualized within the lysosomes with minimal background staining see Figure 11. The final protocol (see page 60) for looking at the TPP1 protein within mouse brain is now routinely used in our lab for studying localization, spread and efficacy of our on-going protein replacement therapies. Future studies in the lab we are interested in include ways to evaluate the therapeutic levels of TPP1 that are needed in treatment of LINCL. For this, an inducible mouse model where

TPP1 can be regulated will be developed. This will help in answering questions on whether LINCL could be reversed or halted after onset of disease. For these studies, the optimized protocol used for IHC will be of use in looking at levels of expression seen when supplementation of the enzyme is accomplished within the mouse. This will be of great use in providing a benchmark for a dosing and treatment regime to be used in clinical trials in patients with this devastating disease.

For the NPC1 protein, an antibody (Novus Bio NPC1), which was previously only used to visualize the protein using western blotting, has now been optimized for use in IHC of the mouse brain (see protocol on page 61). This antibody was chosen as the best antibody from a number of possible candidates (Table 3) because it yielded the most specific signal when comparing staining in the wild-type mouse to that of the knockout. The best results were yielded with a 4% PFA intracardiac perfusion and a 4% PFA post-fix of the tissues using the Novus Biologicals NPC1 antibody. This was done using 1:200 dilution with high salt (500mM KCl) in the blocking buffer. HIER yielded no significant difference (results were comparable with and without it) see Figure 12.

A number of NPC2 antibodies that were isolated in our lab were tested and narrowed down to one antibody for studying the localization of NPC2 within the mouse brain (Table 3). Best results were achieved with a Bouins intracardiac perfusion paired with a Bouins post-fixation of the tissue. The affinity purified NPC2 antibody HL5873 at a dilution of 1:800 used with a high salt (500mM KCl) blocking buffer and HIER seemed to give the most specific results (see final protocol page 62) and Figure 13.

Optimization of these IHC protocols was an important and necessary step for the advancement of our understanding of these lysosomal proteins and where they are expressed throughout the mouse brain. It is unfortunate that the optimum conditions for NPC1 and NPC2 differed greatly and therefore these proteins could not be visualized simultaneously at this time. This would have been a very useful tool for looking at how these proteins co-localize throughout the mouse brain.

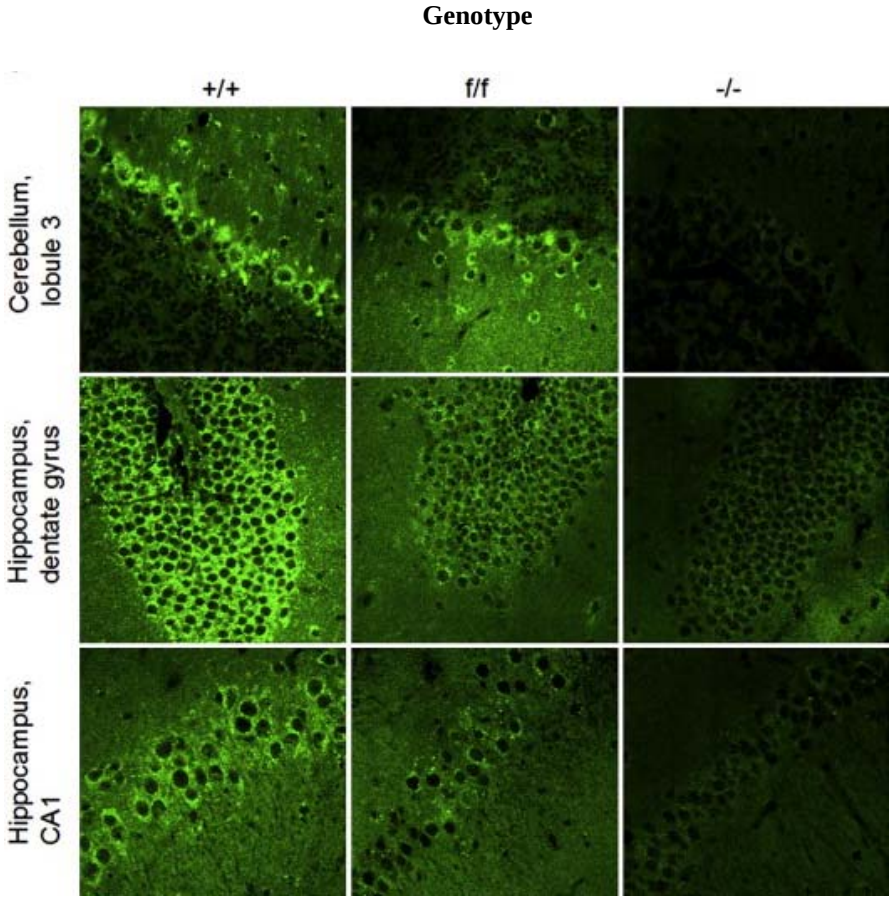

Figure 11: From (Sleat et al., 2008)Immunohistochemical detection of TPP 1 in sections from cerebellum and hippocampus (CA1 region and dentate gyrus) using a rabbit polyclonal anti-TPPI antibody and visualized using a fluorescent-labeled secondary antibody. Mice were between 52 and 57 days of age and multiple sections were examined from independent duplicates for each genotype before selection of representative images. Images were acquired using a Zeiss LSM-410 confocal laser scanning microscope using a 63× oil objective. All mice were congenic for the C57BL/6 strain background.

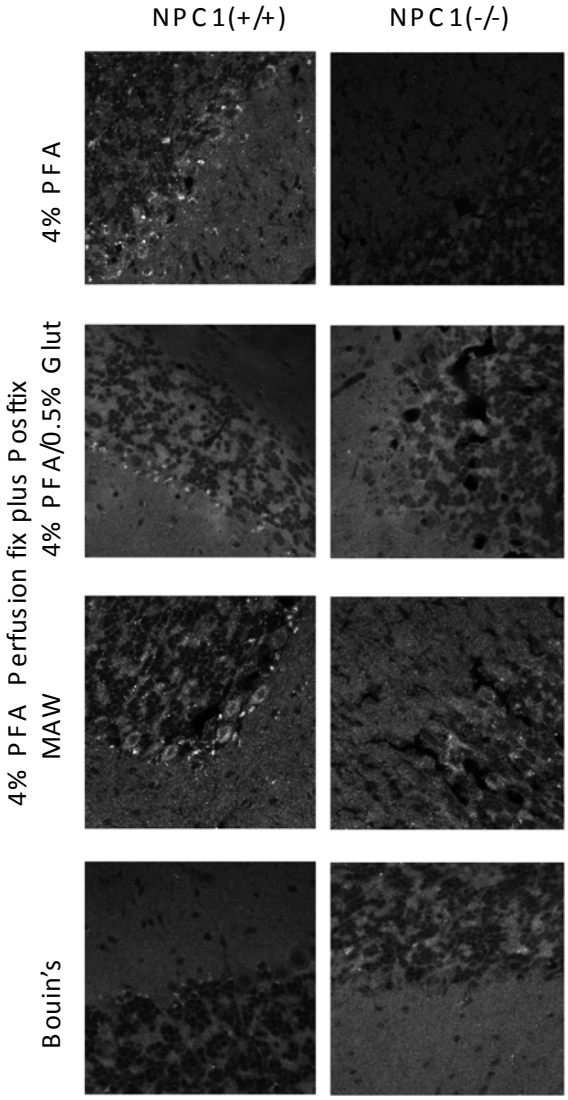

Figure 12: NPC1 antibody Novus Biologicals optimization of intracardiac perfusion and post-fixative. 4% PFA perfusion fix plus various post-fixes as shown above Left side is the wild-type mouse cerebellar sections compared with the knockout NPC1 cerebellar sections. 63x oil objective

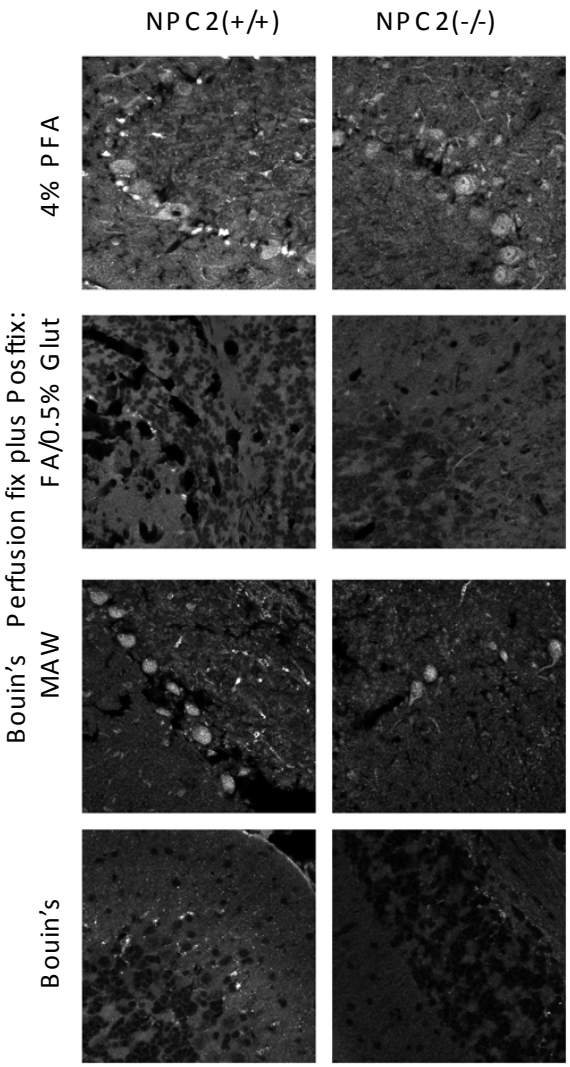

Figure 13: NPC2 antibody HL5873 optimization of intracardiac perfusion and post-fixative. Bouins perfusion fix plus various post-fixes as shown above Left side is the wild-type mouse cerebellar sections compared with the knockout NPC2 cerebellar sections. 63x oil objective

Appendix

TPP1 Protocol

Slide Preparation

Bouins intracardiac perfusion for 10min @ rate 18ml/min (#7 on perfusion pump) with post fix conditions as follows:

1. **Drop-fix of brains (halved) in Bouins o/n**
2. Switch all tissues to 1x PBS x3 to clear post fix
3. Sink tissues in 15% Sucrose in PBS O/N or for up to 48hrs at 4C **(change frequently till yellow color is gone when using Bouins)**
4. Sink tissues in 30% Sucrose in PBS O/N or for up to 48hrs at 4C **(change frequently till yellow color is gone when using Bouins)**
5. Embed in M-1 Shandon Embedding or OCT in a 2-methylbutane bath on dry ice. *Steps 3-4 are done in the cold room while on end over end shaker.*
6. Cut sections use superfrost plus slides- 10 micron sections, 3sections/slide
    a. Use a drop of 1x PBS pH 7.5 on slide and carefully touch section to drop of water (without touching stage) to allow for section to spread
    b. Air-dry O/N or (4C with dessicator)
    c. Place in a slide holder with a dessicator at –80C for longer storage

TPP1 Antibody Staining

7. Thaw frozen slides at 4C before use for 1hr-O/N or at room temp for 20min or till condensation is gone and slide is dry.
8. Wash slides 3xPBS
9. Permeabilize with 0.5% TritonX100/PBS 10min
10. **Block with 3% BSA/500mM NaCl/0.2% Tween20/PBS 30min**
11. **Add primary antibody R72 1:100 dilution in blocking buffer, spin down to get rid of aggregates at 20,000RCF for 10min, add to sections and incubate at RT for 1hr**
12. Wash with 1% TritonX100/PBS 4x
13. Add 1x blocking solution for 5min
14. Add secondary Ab AlexaFluor488 green @ 1:400 (co. recommended) dilution, spin down to get rid of aggregates at 20,000RCF for 10min, add to sections and incubate at RT for 1hr in a light protected container
15. Light protect and wash with 1% TritonX100/PBS 4x
16. Light Protect and wash with PBS 2x and H_2O 1x briefly before mounting and sealing using antifade aqueous mounting glue for fluorescence

NPC1 Protocol

Slide Preparation

4% PFA intracardiac perfusion for 10min @ rate 18ml/min (#7 on perfusion pump) with post fix conditions as follows:

1. **Drop-fix of brains (halved) in 4% PFA o/n**
2. Switch all tissues to 1x PBS x3 to clear post fix
3. Sink tissues in 15% Sucrose in PBS O/N or for up to 48hrs at 4C
4. Sink tissues in 30% Sucrose in PBS O/N or for up to 48hrs at 4C
5. Embed in M-1 Shandon Embedding or OCT in a 2-methylbutane bath on dry ice. *Steps 3-4 are done in the cold room while on end over end shaker.*
6. Cut sections use superfrost plus slides- 10 micron sections, 3sections/slide
    a. Use a drop of 1x PBS pH 7.5 on slide and carefully touch section to drop of water (without touching stage) to allow for section to spread
    b. Air-dry O/N or (4C with dessicator)
    c. Place in a slide holder with a dessicator at –80C for longer storage

NPC1 Antibody Staining

7. Thaw frozen slides at 4C before use for 1hr-O/N or at room temp for 20min or till condensation is gone and slide is dry.
8. Wash slides 3xPBS
9. Permeabilize with 0.5% TritonX100/PBS 10min
10. **Block with 3% BSA/500mM KCl/0.2% Tween20/PBS 30min**
11. **Add primary antibody Novus Bio NPC1 1:200 dilution in blocking buffer, spin down to get rid of aggregates at 20,000RCF for 10min, add to sections and incubate at RT for 1hr**
12. Wash with 1% TritonX100/PBS 4x
13. Add 1x blocking solution for 5min
14. Add secondary Ab AlexaFluor488 green @ 1:400 (co. recommended) dilution, spin down to get rid of aggregates at 20,000RCF for 10min, add to sections and incubate at RT for 1hr in a light protected container
15. Light protect and wash with 1% TritonX100/PBS 4x
16. Light Protect and wash with PBS 2x and H_2O 1x briefly before mounting and sealing using antifade aqueous mounting glue for fluorescence

NPC2 Protocol

Slide Preparation

Bouins intracardiac perfusion for 10min @ rate 18ml/min (#7 on perfusion pump) with post fix conditions as follows:

1. **Drop-fix of brains (halved) in Bouins o/n**
2. Switch all tissues to 1x PBS x3 to clear post fix
3. Sink tissues in 15% Sucrose in PBS O/N or for up to 48hrs at 4C **(change frequently till yellow color is gone when using Bouins)**
4. Sink tissues in 30% Sucrose in PBS O/N or for up to 48hrs at 4C **(change frequently till yellow color is gone when using Bouins)**
5. Embed in M-1 Shandon Embedding or OCT in a 2-methylbutane bath on dry ice. *Steps 3-4 are done in the cold room while on end over end shaker.*
6. Cut sections use superfrost plus slides- 10 micron sections, 3sections/slide
    a. Use a drop of 1x PBS pH 7.5 on slide and carefully touch section to drop of water (without touching stage) to allow for section to spread
    b. Air-dry O/N or (4C with dessicator)
    c. Place in a slide holder with a dessicator at –80C for longer storage

NPC2 Antibody Staining

7. Thaw frozen slides at 4C before use for 1hr-O/N or at room temp for 20min or till condensation is gone and slide is dry.
8. Wash slides 3xPBS
9. **Fill glass staining slide chambers with Antigen Unmasking Solution (Citrate Salt Based) H-3300 and micro wave until boiling. Insert slides into boiled solution for 30 minutes**
10. Permeabilize with 0.5% TritonX100/PBS 10min
11. **Block with 3% BSA/500mM KCl/0.2% Tween20/PBS 30min**
12. **Add primary antibody HL5873 1:800 dilution in blocking buffer, spin down to get rid of aggregates at 20,000RCF for 10min, add to sections and incubate at RT for 1hr**
13. Wash with 1% TritonX100/PBS 4x
14. Add 1x blocking solution for 5min
15. Add secondary Ab AlexaFluor488 green @ 1:400 (co. recommended) dilution, spin down to get rid of aggregates at 20,000RCF for 10min, add to sections and incubate at RT for 1hr in a light protected container
16. Light protect and wash with 1% TritonX100/PBS 4x
17. Light Protect and wash with PBS 2x and H_2O 1x briefly before mounting and sealing using antifade aqueous mounting glue for fluorescence

BIBLIOGRAPHY

Bosch, A., E. Perret, N. Desmaris, and J.M. Heard. 2000. Long-term and significant correction of brain lesions in adult mucopolysaccharidosis type VII mice using recombinant AAV vectors. *Mol Ther*. 1:63-70.

Brady, R.O., J.N. Kanfer, M.B. Mock, and D.S. Fredrickson. 1966. The metabolism of sphingomyelin. II. Evidence of an enzymatic deficiency in Niemann-Pick diseae. *Proc Natl Acad Sci U S A*. 55:366-9.

Brown, D., J. Lydon, M. McLaughlin, A. Stuart-Tilley, R. Tyszkowski, and S. Alper. 1996. Antigen retrieval in cryostat tissue sections and cultured cells by treatment with sodium dodecyl sulfate (SDS). *Histochem Cell Biol*. 105:261-7.

Brown, M.S., and J.L. Goldstein. 1985. The LDL receptor and HMG-CoA reductase--two membrane molecules that regulate cholesterol homeostasis. *Curr Top Cell Regul*. 26:3-15.

Bruni, S., L. Loschi, C. Incerti, O. Gabrielli, and G.V. Coppa. 2007. Update on treatment of lysosomal storage diseases. *Acta Myol*. 26:87-92.

Cabrera-Salazar, M.A., E.M. Roskelley, J. Bu, B.L. Hodges, N. Yew, J.C. Dodge, L.S. Shihabuddin, I. Sohar, D.E. Sleat, R.K. Scheule, B.L. Davidson, S.H. Cheng, P. Lobel, and M.A. Passini. 2007. Timing of therapeutic intervention determines functional and survival outcomes in a mouse model of late infantile batten disease. *Mol Ther*. 15:1782-8.

Carstea, E.D., J.A. Morris, K.G. Coleman, S.K. Loftus, D. Zhang, C. Cummings, J. Gu, M.A. Rosenfeld, W.J. Pavan, D.B. Krizman, J. Nagle, M.H. Polymeropoulos, S.L. Sturley, Y.A. Ioannou, M.E. Higgins, M. Comly, A. Cooney, A. Brown, C.R. Kaneski, E.J. Blanchette-Mackie, N.K. Dwyer, E.B. Neufeld, T.Y. Chang, L. Liscum, J.F. Strauss, 3rd, K. Ohno, M. Zeigler, R. Carmi, J. Sokol, D. Markie, R.R. O'Neill, O.P. van Diggelen, M. Elleder, M.C. Patterson, R.O. Brady, M.T. Vanier, P.G. Pentchev, and D.A. Tagle. 1997. Niemann-Pick C1 disease gene: homology to mediators of cholesterol homeostasis. *Science*. 277:228-31.

Cheruku, S.R., Z. Xu, R. Dutia, P. Lobel, and J. Storch. 2006. Mechanism of cholesterol transfer from the Niemann-Pick type C2 protein to model membranes supports a role in lysosomal cholesterol transport. *J Biol Chem*. 281:31594-604.

Clarke, J.T., and R.M. Iwanochko. 2005. Enzyme replacement therapy of Fabry disease. *Mol Neurobiol*. 32:43-50.

Cooper, J.D., C. Russell, and H.M. Mitchison. 2006. Progress towards understanding disease mechanisms in small vertebrate models of neuronal ceroid lipofuscinosis. *Biochim Biophys Acta*. 1762:873-89.

Crawley, J.N. 2000. What's wrong with my mouse? : behavioral phenotyping of transgenic and knockout mice. Wiley-Liss, New York. xiii, 329 p. pp.

Cruz, J.C., S. Sugii, C. Yu, and T.Y. Chang. 2000. Role of Niemann-Pick type C1 protein in intracellular trafficking of low density lipoprotein-derived cholesterol. *J Biol Chem*. 275:4013-21.

Davies, J.P., F.W. Chen, and Y.A. Ioannou. 2000. Transmembrane molecular pump activity of Niemann-Pick C1 protein. *Science*. 290:2295-8.

de Vries, W.N., L.T. Binns, K.S. Fancher, J. Dean, R. Moore, R. Kemler, and B.B. Knowles. 2000. Expression of Cre recombinase in mouse oocytes: a means to study maternal effect genes. *Genesis*. 26:110-2.

Distl, R., S. Treiber-Held, F. Albert, V. Meske, K. Harzer, and T.G. Ohm. 2003. Cholesterol storage and tau pathology in Niemann-Pick type C disease in the brain. *J Pathol*. 200:104-11.

Elleder, M., and J. Tyynela. 1998. Incidence of neuronal perikaryal spheroids in neuronal ceroid lipofuscinoses (Batten disease). *Clin Neuropathol*. 17:184-9.

Erickson, R.P., W.S. Garver, F. Camargo, G.S. Hossain, and R.A. Heidenreich. 2000. Pharmacological and genetic modifications of somatic cholesterol do not substantially alter the course of CNS disease in Niemann-Pick C mice. *J Inherit Metab Dis*. 23:54-62.

Franco, D., P.A. de Boer, C. de Gier-de Vries, W.H. Lamers, and A.F. Moorman. 2001. Methods on in situ hybridization, immunohistochemistry and beta-galactosidase reporter gene detection. *Eur J Morphol*. 39:3-25.

Friedland, N., H.L. Liou, P. Lobel, and A.M. Stock. 2003. Structure of a cholesterol-binding protein deficient in Niemann-Pick type C2 disease. *Proc Natl Acad Sci U S A*. 100:2512-7.

Frisella, W.A., L.H. O'Connor, C.A. Vogler, M. Roberts, S. Walkley, B. Levy, T.M. Daly, and M.S. Sands. 2001. Intracranial injection of recombinant adeno-associated virus improves cognitive function in a murine model of mucopolysaccharidosis type VII. *Mol Ther*. 3:351-8.

Goodrum, J.F., and P.G. Pentchev. 1997. Cholesterol reutilization during myelination of regenerating PNS axons is impaired in Niemann-Pick disease type C mice. *J Neurosci Res*. 49:389-92.

Griffin, L.D., W. Gong, L. Verot, and S.H. Mellon. 2004. Niemann-Pick type C disease involves disrupted neurosteroidogenesis and responds to allopregnanolone. *Nat Med*. 10:704-11.

Haltia, M. 2003. The neuronal ceroid-lipofuscinoses. *J Neuropathol Exp Neurol*. 62:1-13.

Haskell, R.E., S.M. Hughes, J.A. Chiorini, J.M. Alisky, and B.L. Davidson. 2003. Viral-mediated delivery of the late-infantile neuronal ceroid lipofuscinosis gene, TPP-I to the mouse central nervous system. *Gene Ther*. 10:34-42.

Higashi, Y., S. Murayama, P.G. Pentchev, and K. Suzuki. 1993. Cerebellar degeneration in the Niemann-Pick type C mouse. *Acta Neuropathol*. 85:175-84.

Higgins, M.E., J.P. Davies, F.W. Chen, and Y.A. Ioannou. 1999. Niemann-Pick C1 is a late endosome-resident protein that transiently associates with lysosomes and the trans-Golgi network. *Mol Genet Metab*. 68:1-13.

Hobert, J.A., and G. Dawson. 2006. Neuronal ceroid lipofuscinoses therapeutic strategies: past, present and future. *Biochim Biophys Acta*. 1762:945-53.

Ikonen, E., and M. Holtta-Vuori. 2004. Cellular pathology of Niemann-Pick type C disease. *Semin Cell Dev Biol*. 15:445-54.

Infante, R.E., A. Radhakrishnan, L. Abi-Mosleh, L.N. Kinch, M.L. Wang, N.V. Grishin, J.L. Goldstein, and M.S. Brown. 2008. Purified NPC1 protein: II. Localization of sterol binding to a 240-amino acid soluble luminal loop. *J Biol Chem*. 283:1064-75.

Ino, H. 2003. Antigen retrieval by heating en bloc for pre-fixed frozen material. *J Histochem Cytochem*. 51:995-1003.

Karten, B., D.E. Vance, R.B. Campenot, and J.E. Vance. 2002. Cholesterol accumulates in cell bodies, but is decreased in distal axons, of Niemann-Pick C1-deficient neurons. *J Neurochem*. 83:1154-63.

Klunemann, H.H., M. Elleder, W.E. Kaminski, K. Snow, J.M. Peyser, J.F. O'Brien, D. Munoz, G. Schmitz, H.E. Klein, and W.W. Pendlebury. 2002. Frontal lobe atrophy due to a mutation in the cholesterol binding protein HE1/NPC2. *Ann Neurol*. 52:743-9.

Ko, D.C., J. Binkley, A. Sidow, and M.P. Scott. 2003. The integrity of a cholesterol-binding pocket in Niemann-Pick C2 protein is necessary to control lysosome cholesterol levels. *Proc Natl Acad Sci U S A*. 100:2518-25.

Kobayashi, T., M.H. Beuchat, M. Lindsay, S. Frias, R.D. Palmiter, H. Sakuraba, R.G. Parton, and J. Gruenberg. 1999. Late endosomal membranes rich in lysobisphosphatidic acid regulate cholesterol transport. *Nat Cell Biol*. 1:113-8.

Lake, B.D., and N.A. Hall. 1993. Immunolocalization studies of subunit c in late-infantile and juvenile Batten disease. *J Inherit Metab Dis*. 16:263-6.

Lin, L., and P. Lobel. 2001. Production and characterization of recombinant human CLN2 protein for enzyme-replacement therapy in late infantile neuronal ceroid lipofuscinosis. *Biochem J*. 357:49-55.

Lin, L., I. Sohar, H. Lackland, and P. Lobel. 2001. The human CLN2 protein/tripeptidyl-peptidase I is a serine protease that autoactivates at acidic pH. *J Biol Chem*. 276:2249-55.

Liscum, L., R.M. Ruggiero, and J.R. Faust. 1989. The intracellular transport of low density lipoprotein-derived cholesterol is defective in Niemann-Pick type C fibroblasts. *J Cell Biol*. 108:1625-36.

Liu, B., S.D. Turley, D.K. Burns, A.M. Miller, J.J. Repa, and J.M. Dietschy. 2009. Reversal of defective lysosomal transport in NPC disease ameliorates liver dysfunction and neurodegeneration in the npc1-/- mouse. *Proc Natl Acad Sci U S A*. 106:2377-82.

Lund, E.G., C. Xie, T. Kotti, S.D. Turley, J.M. Dietschy, and D.W. Russell. 2003. Knockout of the cholesterol 24-hydroxylase gene in mice reveals a brain-specific mechanism of cholesterol turnover. *J Biol Chem*. 278:22980-8.

Matalon, R., S. Surendran, P.L. Rady, M.J. Quast, G.A. Campbell, K.M. Matalon, S.K. Tyring, J. Wei, C.S. Peden, E.L. Ezell, N. Muzyczka, and R.J. Mandel. 2003. Adeno-associated virus-mediated aspartoacylase gene transfer to the brain of knockout mouse for canavan disease. *Mol Ther*. 7:580-7.

Miyawaki, S., H. Yoshida, S. Mitsuoka, H. Enomoto, and S. Ikehara. 1986. A mouse model for Niemann-Pick disease. Influence of genetic background on disease expression in spm/spm mice. *J Hered*. 77:379-84.

Mukherjee, S., and F.R. Maxfield. 2004. Lipid and cholesterol trafficking in NPC. *Biochim Biophys Acta*. 1685:28-37.

Naureckiene, S., D.E. Sleat, H. Lackland, A. Fensom, M.T. Vanier, R. Wattiaux, M. Jadot, and P. Lobel. 2000. Identification of HE1 as the second gene of Niemann-Pick C disease. *Science*. 290:2298-301.

Neufeld, E.B., M. Wastney, S. Patel, S. Suresh, A.M. Cooney, N.K. Dwyer, C.F. Roff, K. Ohno, J.A. Morris, E.D. Carstea, J.P. Incardona, J.F. Strauss, 3rd, M.T. Vanier, M.C. Patterson, R.O. Brady, P.G. Pentchev, and E.J. Blanchette-Mackie. 1999. The Niemann-Pick C1 protein resides in a vesicular compartment linked to retrograde transport of multiple lysosomal cargo. *J Biol Chem*. 274:9627-35.

Neufeld, E.F. 1991. Lysosomal storage diseases. *Annu Rev Biochem*. 60:257-80.

Okamura, N., S. Kiuchi, M. Tamba, T. Kashima, S. Hiramoto, T. Baba, F. Dacheux, J.L. Dacheux, Y. Sugita, and Y.Z. Jin. 1999. A porcine homolog of the major secretory protein of human epididymis, HE1, specifically binds cholesterol. *Biochim Biophys Acta*. 1438:377-87.

Palmer, D.N., I.M. Fearnley, J.E. Walker, N.A. Hall, B.D. Lake, L.S. Wolfe, M. Haltia, R.D. Martinus, and R.D. Jolly. 1992. Mitochondrial ATP synthase subunit c storage in the ceroid-lipofuscinoses (Batten disease). *Am J Med Genet*. 42:561-7.

Passini, M.A., J.C. Dodge, J. Bu, W. Yang, Q. Zhao, D. Sondhi, N.R. Hackett, S.M. Kaminsky, Q. Mao, L.S. Shihabuddin, S.H. Cheng, D.E. Sleat, G.R. Stewart, B.L. Davidson, P. Lobel, and R.G. Crystal. 2006. Intracranial delivery of CLN2 reduces brain pathology in a mouse model of classical late infantile neuronal ceroid lipofuscinosis. *J Neurosci*. 26:1334-42.

Passini, M.A., S.L. Macauley, M.R. Huff, T.V. Taksir, J. Bu, I.H. Wu, P.A. Piepenhagen, J.C. Dodge, L.S. Shihabuddin, C.R. O'Riordan, E.H. Schuchman, and G.R. Stewart. 2005. AAV vector-mediated correction of brain pathology in a mouse model of Niemann-Pick A disease. *Mol Ther*. 11:754-62.

Passini, M.A., D.J. Watson, C.H. Vite, D.J. Landsburg, A.L. Feigenbaum, and J.H. Wolfe. 2003. Intraventricular brain injection of adeno-associated virus type 1 (AAV1) in neonatal mice results in complementary patterns of neuronal transduction to AAV2 and total long-term correction of storage lesions in the brains of beta-glucuronidase-deficient mice. *J Virol*. 77:7034-40.

Patterson, M.C., and F. Platt. 2004. Therapy of Niemann-Pick disease, type C. *Biochim Biophys Acta*. 1685:77-82.

Pentchev, P.G. 2004. Niemann-Pick C research from mouse to gene. *Biochim Biophys Acta*. 1685:3-7.

Pentchev, P.G., A.D. Boothe, H.S. Kruth, H. Weintroub, J. Stivers, and R.O. Brady. 1984. A genetic storage disorder in BALB/C mice with a metabolic block in esterification of exogenous cholesterol. *J Biol Chem*. 259:5784-91.

Ponder, K.P., and M.E. Haskins. 2007. Gene therapy for mucopolysaccharidosis. *Expert Opin Biol Ther*. 7:1333-45.

Puri, V., J.R. Jefferson, R.D. Singh, C.L. Wheatley, D.L. Marks, and R.E. Pagano. 2003. Sphingolipid storage induces accumulation of intracellular cholesterol by stimulating SREBP-1 cleavage. *J Biol Chem*. 278:20961-70.

Puri, V., R. Watanabe, M. Dominguez, X. Sun, C.L. Wheatley, D.L. Marks, and R.E. Pagano. 1999. Cholesterol modulates membrane traffic along the endocytic pathway in sphingolipid-storage diseases. *Nat Cell Biol*. 1:386-8.

Ramos-Vara, J.A. 2005. Technical aspects of immunohistochemistry. *Vet Pathol*. 42:405-26.

Rawlings, N.D., and A.J. Barrett. 1999. Tripeptidyl-peptidase I is apparently the CLN2 protein absent in classical late-infantile neuronal ceroid lipofuscinosis. *Biochim Biophys Acta*. 1429:496-500.

Rider, J.A., and D.L. Rider. 1988. Batten disease: past, present, and future. *Am J Med Genet Suppl*. 5:21-6.

Rogers, A.B., K.S. Cormier, and J.G. Fox. 2006. Thiol-reactive compounds prevent nonspecific antibody binding in immunohistochemistry. *Lab Invest*. 86:526-33.

Sferra, T.J., G. Qu, D. McNeely, R. Rennard, K.R. Clark, W.D. Lo, and P.R. Johnson. 2000. Recombinant adeno-associated virus-mediated correction of lysosomal storage within the central nervous system of the adult mucopolysaccharidosis type VII mouse. *Hum Gene Ther*. 11:507-19.

Sharp, J.D., R.B. Wheeler, B.D. Lake, M. Savukoski, I.E. Jarvela, L. Peltonen, R.M. Gardiner, and R.E. Williams. 1997. Loci for classical and a variant late infantile neuronal ceroid lipofuscinosis map to chromosomes 11p15 and 15q21-23. *Hum Mol Genet*. 6:591-5.

Skorupa, A.F., K.J. Fisher, J.M. Wilson, M.K. Parente, and J.H. Wolfe. 1999. Sustained production of beta-glucuronidase from localized sites after AAV vector gene transfer results in widespread distribution of enzyme and reversal of lysosomal storage lesions in a large volume of brain in mucopolysaccharidosis VII mice. *Exp Neurol*. 160:17-27.

Sleat, D.E., R.J. Donnelly, H. Lackland, C.G. Liu, I. Sohar, R.K. Pullarkat, and P. Lobel. 1997. Association of mutations in a lysosomal protein with classical late-infantile neuronal ceroid lipofuscinosis. *Science*. 277:1802-5.

Sleat, D.E., M. El-Banna, I. Sohar, K.H. Kim, K. Dobrenis, S.U. Walkley, and P. Lobel. 2008. Residual levels of tripeptidyl-peptidase I activity dramatically ameliorate disease in late-infantile neuronal ceroid lipofuscinosis. *Mol Genet Metab*.

Sleat, D.E., R.M. Gin, I. Sohar, K. Wisniewski, S. Sklower-Brooks, R.K. Pullarkat, D.N. Palmer, T.J. Lerner, R.M. Boustany, P. Uldall, A.N. Siakotos, R.J. Donnelly, and P. Lobel. 1999. Mutational analysis of the defective protease in classic late-infantile neuronal ceroid lipofuscinosis, a neurodegenerative lysosomal storage disorder. *Am J Hum Genet*. 64:1511-23.

Sleat, D.E., J.A. Wiseman, M. El-Banna, K.H. Kim, Q. Mao, S. Price, S.L. Macauley, R.L. Sidman, M.M. Shen, Q. Zhao, M.A. Passini, B.L. Davidson, G.R. Stewart, and P. Lobel. 2004a. A mouse model of classical late-infantile neuronal ceroid lipofuscinosis based on targeted disruption of the CLN2 gene results in a loss of tripeptidyl-peptidase I activity and progressive neurodegeneration. *J Neurosci*. 24:9117-26.

Sleat, D.E., J.A. Wiseman, M. El-Banna, S.M. Price, L. Verot, M.M. Shen, G.S. Tint, M.T. Vanier, S.U. Walkley, and P. Lobel. 2004b. Genetic evidence for nonredundant functional cooperativity between NPC1 and NPC2 in lipid transport. *Proc Natl Acad Sci U S A*. 101:5886-91.

Sokol, J., J. Blanchette-Mackie, H.S. Kruth, N.K. Dwyer, L.M. Amende, J.D. Butler, E. Robinson, S. Patel, R.O. Brady, M.E. Comly, and et al. 1988. Type C Niemann-Pick disease. Lysosomal accumulation and defective intracellular mobilization of low density lipoprotein cholesterol. *J Biol Chem*. 263:3411-7.

Sondhi, D., N.R. Hackett, D.A. Peterson, J. Stratton, M. Baad, K.M. Travis, J.M. Wilson, and R.G. Crystal. 2007. Enhanced survival of the LINCL mouse following CLN2 gene transfer using the rh.10 rhesus macaque-derived adeno-associated virus vector. *Mol Ther*. 15:481-91.

Sondhi, D., D.A. Peterson, A.M. Edelstein, K. del Fierro, N.R. Hackett, and R.G. Crystal. 2008. Survival advantage of neonatal CNS gene transfer for late infantile neuronal ceroid lipofuscinosis. *Exp Neurol*. 213:18-27.

Sondhi, D., D.A. Peterson, E.L. Giannaris, C.T. Sanders, B.S. Mendez, B. De, A.B. Rostkowski, B. Blanchard, K. Bjugstad, J.R. Sladek, Jr., D.E. Redmond, Jr., P.L. Leopold, S.M. Kaminsky, N.R. Hackett, and R.G. Crystal. 2005. AAV2-mediated CLN2 gene transfer to rodent and non-human primate brain results in long-term TPP-I expression compatible with therapy for LINCL. *Gene Ther*. 12:1618-32.

Spady, D.K., and J.M. Dietschy. 1983. Sterol synthesis in vivo in 18 tissues of the squirrel monkey, guinea pig, rabbit, hamster, and rat. *J Lipid Res*. 24:303-15.

Storch, J., and Z. Xu. 2009. Niemann-Pick C2 (NPC2) and intracellular cholesterol trafficking. *Biochim Biophys Acta*.

Takikita, S., T. Fukuda, I. Mohri, T. Yagi, and K. Suzuki. 2004. Perturbed myelination process of premyelinating oligodendrocyte in Niemann-Pick type C mouse. *J Neuropathol Exp Neurol*. 63:660-73.

Tashiro, Y., T. Yamazaki, Y. Shimada, Y. Ohno-Iwashita, and K. Okamoto. 2004. Axon-dominant localization of cell-surface cholesterol in cultured hippocampal neurons and its disappearance in Niemann-Pick type C model cells. *Eur J Neurosci*. 20:2015-21.

te Vruchte, D., E. Lloyd-Evans, R.J. Veldman, D.C. Neville, R.A. Dwek, F.M. Platt, W.J. van Blitterswijk, and D.J. Sillence. 2004. Accumulation of glycosphingolipids in Niemann-Pick C disease disrupts endosomal transport. *J Biol Chem*. 279:26167-75.

Turley, S.D., D.K. Burns, C.R. Rosenfeld, and J.M. Dietschy. 1996. Brain does not utilize low density lipoprotein-cholesterol during fetal and neonatal development in the sheep. *J Lipid Res*. 37:1953-61.

Tyynela, J., M. Baumann, M. Henseler, K. Sandhoff, and M. Haltia. 1995. Sphingolipid activator proteins in the neuronal ceroid-lipofuscinoses: an immunological study. *Acta Neuropathol*. 89:391-8.

Tyynela, J., J. Suopanki, M. Baumann, and M. Haltia. 1997. Sphingolipid activator proteins (SAPs) in neuronal ceroid lipofuscinoses (NCL). *Neuropediatrics*. 28:49-52.

Vance, J.E. 2006. Lipid imbalance in the neurological disorder, Niemann-Pick C disease. *FEBS Lett*. 580:5518-24.

Vanier, M.T. 1983. Biochemical studies in Niemann-Pick disease. I. Major sphingolipids of liver and spleen. *Biochim Biophys Acta*. 750:178-84.

Vanier, M.T., and G. Millat. 2004. Structure and function of the NPC2 protein. *Biochim Biophys Acta*. 1685:14-21.

Vines, D.J., and M.J. Warburton. 1999. Classical late infantile neuronal ceroid lipofuscinosis fibroblasts are deficient in lysosomal tripeptidyl peptidase I. *FEBS Lett*. 443:131-5.

Walkley, S.U., and K. Suzuki. 2004. Consequences of NPC1 and NPC2 loss of function in mammalian neurons. *Biochim Biophys Acta*. 1685:48-62.

Watanabe, Y., S. Akaboshi, G. Ishida, T. Takeshima, T. Yano, M. Taniguchi, K. Ohno, and K. Nakashima. 1998. Increased levels of GM2 ganglioside in fibroblasts from a patient with juvenile Niemann-Pick disease type C. *Brain Dev*. 20:95-7.

Watari, H., E.J. Blanchette-Mackie, N.K. Dwyer, J.M. Glick, S. Patel, E.B. Neufeld, R.O. Brady, P.G. Pentchev, and J.F. Strauss, 3rd. 1999a. Niemann-Pick C1 protein: obligatory roles for N-terminal domains and lysosomal targeting in cholesterol mobilization. *Proc Natl Acad Sci U S A*. 96:805-10.

Watari, H., E.J. Blanchette-Mackie, N.K. Dwyer, M. Watari, C.G. Burd, S. Patel, P.G. Pentchev, and J.F. Strauss, 3rd. 2000. Determinants of NPC1 expression and action: key promoter regions, posttranscriptional control, and the importance of a "cysteine-rich" loop. *Exp Cell Res*. 259:247-56.

Watari, H., E.J. Blanchette-Mackie, N.K. Dwyer, M. Watari, E.B. Neufeld, S. Patel, P.G. Pentchev, and J.F. Strauss, 3rd. 1999b. Mutations in the leucine zipper motif and sterol-sensing domain inactivate the Niemann-Pick C1 glycoprotein. *J Biol Chem*. 274:21861-6.

Winchester, B., A. Vellodi, and E. Young. 2000. The molecular basis of lysosomal storage diseases and their treatment. *Biochem Soc Trans*. 28:150-4.

Wisniewski, K.E., E. Kida, A.A. Golabek, W. Kaczmarski, F. Connell, and N. Zhong. 2001. Neuronal ceroid lipofuscinoses: classification and diagnosis. *Adv Genet*. 45:1-34.

Worgall, S., D. Sondhi, N.R. Hackett, B. Kosofsky, M.V. Kekatpure, N. Neyzi, J.P. Dyke, D. Ballon, L. Heier, B.M. Greenwald, P. Christos, M. Mazumdar, M.M.

Souweidane, M.G. Kaplitt, and R.G. Crystal. 2008. Treatment of late infantile neuronal ceroid lipofuscinosis by CNS administration of a serotype 2 adeno-associated virus expressing CLN2 cDNA. *Hum Gene Ther*. 19:463-74.

Xie, C., D.K. Burns, S.D. Turley, and J.M. Dietschy. 2000. Cholesterol is sequestered in the brains of mice with Niemann-Pick type C disease but turnover is increased. *J Neuropathol Exp Neurol*. 59:1106-17.

Xie, C., S.D. Turley, and J.M. Dietschy. 1999. Cholesterol accumulation in tissues of the Niemann-pick type C mouse is determined by the rate of lipoprotein-cholesterol uptake through the coated-pit pathway in each organ. *Proc Natl Acad Sci U S A*. 96:11992-7.

Xu, S., B. Benoff, H.L. Liou, P. Lobel, and A.M. Stock. 2007. Structural basis of sterol binding by NPC2, a lysosomal protein deficient in Niemann-Pick type C2 disease. *J Biol Chem*. 282:23525-31.

Zeman, W., and P. Dyken. 1969. Neuronal ceroid-lipofuscinosis (Batten's disease): relationship to amaurotic family idiocy? *Pediatrics*. 44:570-83.

Zervas, M., K. Dobrenis, and S.U. Walkley. 2001a. Neurons in Niemann-Pick disease type C accumulate gangliosides as well as unesterified cholesterol and undergo dendritic and axonal alterations. *J Neuropathol Exp Neurol*. 60:49-64.

Zervas, M., K.L. Somers, M.A. Thrall, and S.U. Walkley. 2001b. Critical role for glycosphingolipids in Niemann-Pick disease type C. *Curr Biol*. 11:1283-7.

Zhang, J., and R.P. Erickson. 2000. A modifier of Niemann Pick C 1 maps to mouse chromosome 19. *Mamm Genome*. 11:69-71.

Zhong, N., K.E. Wisniewski, J. Hartikainen, W. Ju, D.N. Moroziewicz, L. McLendon, S.S. Sklower Brooks, and W.T. Brown. 1998. Two common mutations in the CLN2 gene underlie late infantile neuronal ceroid lipofuscinosis. *Clin Genet*. 54:234-8.